

1                   **NEW TIME DOMAIN DECOMPOSITION METHODS FOR**  
2                   **PARABOLIC OPTIMAL CONTROL PROBLEMS I:**  
3                   **DIRICHLET-NEUMANN AND NEUMANN-DIRICHLET**  
4                   **ALGORITHMS\***

5                   MARTIN J. GANDER<sup>†</sup> AND LIU-DI LU<sup>†</sup>

6                   **Abstract.** We present new Dirichlet-Neumann and Neumann-Dirichlet algorithms with a time  
7 domain decomposition applied to unconstrained parabolic optimal control problems. After a spatial  
8 semi-discretization, we use the Lagrange multiplier approach to derive a coupled forward-backward  
9 optimality system, which can then be solved using a time domain decomposition. Due to the forward-  
10 backward structure of the optimality system, three variants can be found for the Dirichlet-Neumann  
11 and Neumann-Dirichlet algorithms. We analyze their convergence behavior and determine the opti-  
12 mal relaxation parameter for each algorithm. Our analysis reveals that the most natural algorithms  
13 are actually only good smoothers, and there are better choices which lead to efficient solvers. We  
14 illustrate our analysis with numerical experiments.

15                   **Key words.** Time domain decomposition, Dirichlet-Neumann algorithm, Neumann-Dirichlet  
16 algorithm, Parallel in Time, Parabolic optimal control problems, Convergence analysis.

17                   **MSC codes.** 65M12,65M55,65Y05,

18                   **1. Introduction.** PDE-constrained optimal control problems arise in various  
19 areas, often containing multiphysics or multiscale phenomena, and also high frequency  
20 components on different time scales. This requires very fine spatial and temporal  
21 discretizations, resulting in very large problems, for which efficient parallel solvers are  
22 needed; we refer to [14, 26] for a brief review. We present and analyze a new class  
23 of time domain decomposition methods based on Dirichlet-Neumann and Neumann-  
24 Dirichlet techniques. We consider as our model a parabolic optimal control problem:  
25 for a given target function  $\hat{y} \in L^2(Q)$ ,  $\gamma \geq 0$  and  $\nu > 0$ , we want to minimize the cost  
26 functional

27 (1.1)            $J(y, u) := \frac{1}{2} \|y - \hat{y}\|_{L^2(Q)}^2 + \frac{\gamma}{2} \|y(T) - \hat{y}(T)\|_{L^2(\Omega)}^2 + \frac{\nu}{2} \|u\|_{U_{\text{ad}}}^2,$

28 subject to the linear parabolic state equation

29 (1.2)           
$$\begin{aligned} \partial_t y - \Delta y &= u && \text{in } Q := \Omega \times (0, T), \\ y &= 0 && \text{on } \Sigma := \partial\Omega \times (0, T), \\ y(0) &= y_0 && \text{on } \Sigma_0 := \Omega \times \{0\}, \end{aligned}$$

30 where  $\Omega \subset \mathbb{R}^d$ ,  $d = 1, 2, 3$  is a bounded domain with boundary  $\partial\Omega$ , and  $T$  is the fixed  
31 final time. The control  $u$  on the right-hand side of the PDE is in an admissible set  
32  $U_{\text{ad}}$ , and we want to control the solution of the parabolic PDE (1.2) towards a target  
33 state  $\hat{y}$ . For simplicity, we consider here homogeneous boundary conditions.

34                   The parabolic optimal control problem (1.1)-(1.2) has a unique solution for the  
35 classical choice  $u \in L^2(Q)$ , which can be characterized by a forward-backward op-  
36 timality system, see e.g. [4, 18, 26]. More recently, also energy regularization has  
37 been considered, see [23] for elliptic and [16] for parabolic cases. This is motivated by

---

\*Submitted to the editors 2023.07.05.

**Funding:** This work was funded by the Swiss National Science Foundation Grant 192064.

<sup>†</sup>Section de Mathématiques, Université de Genève, rue du Conseil-Général 5-7, CP 64, 1205, Geneva, Switzerland (martin.gander@unige.ch, liudi.lu@unige.ch).

38 the fact that the state  $y \in L^2(0, T; H_0^1(\Omega))$  is well-defined as the solution of the heat  
 39 equation (1.2) for the control  $z \in L^2(0, T; H^{-1}(\Omega))$ , and thus offers an interesting  
 40 alternative.

41 We are interested in applying Time Domain Decomposition methods (DDMs) to  
 42 the forward-backward optimality system. DDMs were developed for elliptic PDEs and  
 43 are very efficient in parallel computing environments, see e.g. [7, 25]. DDMs were ex-  
 44 tended to time-dependent problems using waveform relaxation techniques from [17],  
 45 with a spatial decomposition and solving the problem on small space-time cylin-  
 46 ders [12]. The extension of DDMs to elliptic optimal control problems is quite natural,  
 47 see [1, 2, 5, 9], but less is known about DDMs applied to parabolic optimal control  
 48 problems.

49 The role of the time variable in forward-backward optimality systems is key,  
 50 and it is natural to seek efficient solvers through time domain decomposition. For  
 51 classical evolution problems, the idea of time domain decomposition goes back to [24].  
 52 Parallel Runge Kutta methods were introduced in [22] with good small scale time  
 53 parallelism. In [20, 27], the authors propose to combine multigrid methods with  
 54 waveform relaxation. Parareal [19] uses a different approach, namely multiple shooting  
 55 with an approximate Jacobian on a coarse grid, and Parareal techniques led to a new  
 56 ParaOpt algorithm [10] for optimal control, see also [13]. In [8, 15], Schwarz methods  
 57 are used to decompose the time domain for optimal control. Waveform relaxation  
 58 techniques can also be applied to address such optimal control problems, for instance,  
 59 using Dirichlet-Neumann waveform relaxation methods [21] and Optimized Schwarz  
 60 waveform relaxation methods [6]. Note that the decomposition in [6, 21] is in space  
 61 of the PDE constraint, in contrast to the approach presented in [8, 15], and also in  
 62 contrast to our approach in time here.

63 We develop and analyze here new time domain decomposition algorithms to solve  
 64 the PDE-constrained problem (1.1)-(1.2) using Dirichlet-Neumann and Neumann-  
 65 Dirichlet techniques that go back to [3] for space parallelism. We introduce in Section 2  
 66 the optimality system and its semi-discretization. In Section 3 we present our new  
 67 time parallel Dirichlet-Neumann and Neumann-Dirichlet algorithms and study their  
 68 convergence. Numerical experiments are shown in Section 4, and we draw conclusions  
 69 in Section 5.

70 **2. Optimality system and its semi-discretization.** The PDE-constrained  
 71 optimization problem (1.1)-(1.2) can be solved using Lagrange multipliers [26, Chapter  
 72 3], see also [11] for a historical context. To obtain the associated optimality system,  
 73 we introduce the Lagrangian function  $\mathcal{L}$  associated with Problem (1.1)-(1.2),

$$\begin{aligned}
 \mathcal{L}(y, u, \lambda) &= J(y, u) + \langle \partial_t y - \Delta y - u, \lambda \rangle \\
 &= \int_0^T \left( \langle \partial_t y, \lambda \rangle_{V', V} + \int_{\Omega} \left( \frac{1}{2} |y - \hat{y}|^2 + \frac{\nu}{2} |u|^2 + \nabla y \cdot \nabla \lambda - u \lambda \right) dx \right) dt \\
 &\quad + \frac{\gamma}{2} \int_{\Omega} |y(T) - \hat{y}(T)|^2 dx,
 \end{aligned}$$

75 with  $y \in W(0, T) := L^2(0, T; V) \cap H^1(0, T; V')$ ,  $u \in L^2(Q)$ ,  $V := H_0^1(\Omega)$  and  $V' :=$   
 76  $H^{-1}(\Omega)$  the dual space of  $V$ . Here  $\lambda \in L^2(0, T; V)$  denotes the adjoint state (also  
 77 called the Lagrange multiplier). Taking the derivative of  $\mathcal{L}$  with respect to  $\lambda$  and  
 78 equating this to zero, we find for all test functions  $\chi \in L^2(0, T; V)$ ,

$$0 = \langle \partial_{\lambda} \mathcal{L}(y, u, \lambda), \chi \rangle = \int_0^T \left( \langle \partial_t y, \chi \rangle_{V', V} + \int_{\Omega} (\nabla y \cdot \nabla \chi - u \chi) dx \right) dt,$$

80 which implies that  $y \in V$  is the weak solution of the state equation (1.2) (also called  
81 the primal problem). Taking the derivative of  $\mathcal{L}$  with respect to  $y$  and equating this  
82 to zero, and obtain for all  $\chi \in W(0, T)$

$$\begin{aligned} 0 = \langle \partial_y \mathcal{L}(y, u, \lambda), \chi \rangle &= \int_0^T \left( \langle \partial_t \chi, \lambda \rangle_{V', V} + \int_{\Omega} ((y - \hat{y})\chi + \nabla \chi \cdot \nabla \lambda) \, d\mathbf{x} \right) dt \\ &= \langle \chi(T), \lambda(T) + \gamma(y(T) - \hat{y}(T)) \rangle_{L^2(\Omega)} - \langle \chi(0), \lambda(0) \rangle_{L^2(\Omega)} \\ &\quad + \int_0^T \langle -\partial_t \lambda - \Delta \lambda + (y - \hat{y}), \chi \rangle_{V', V} \, dt, \end{aligned}$$

84 where we used integration by parts with respect to  $t$  in  $\partial_t \chi$  and with respect to  $\mathbf{x}$  in  
85  $\nabla \chi$ . By choosing  $\chi \in C_0^\infty(Q)$  and applying an argument of density, we find that the  
86 last integral is zero. Choosing then  $\chi \in W(0, T)$  such that  $\chi(0) = 0$ , we obtain the  
87 adjoint equation (also called the dual problem)

$$\begin{aligned} (2.1) \quad & \partial_t \lambda + \Delta \lambda = y - \hat{y} && \text{in } Q, \\ & \lambda = 0 && \text{on } \Sigma, \\ & \lambda(T) = -\gamma(y(T) - \hat{y}(T)) && \text{on } \Sigma_T := \Omega \times \{T\}. \end{aligned}$$

89 Finally, taking the derivative of  $\mathcal{L}$  with respect to  $u$  and equating this to zero, we  
90 obtain for all test functions  $\chi \in L^2(Q)$ ,  $0 = \langle \partial_u(y, u, p), \chi \rangle = \int_0^T \int_{\Omega} (\nu u - \lambda)\chi \, d\mathbf{x} \, dt$ ,  
91 which gives the optimality condition

$$(2.2) \quad \lambda = \nu u \quad \text{in } Q.$$

93 If a control  $u$  is optimal with the associated state  $y$  of the optimization problem (1.1)-  
94 (1.2), then the first-order optimality system (1.2), (2.1) and (2.2) must be satisfied.  
95 This is a forward-backward system, i.e., the primal problem is solved forward in time  
96 with an initial condition while the dual problem is solved backward in time with a  
97 final condition, and our new time decomposition algorithms solve this system. Since  
98 the time variable plays a special role, we consider a semi-discretization in space, and  
99 replace the spatial operator  $-\Delta$  in the primal problem (1.2) by a matrix  $A \in \mathbb{R}^{n \times n}$ ,  
100 for instance using a Finite Difference discretization in space. We then obtain as above  
101 the semi-discrete optimality system (dot denoting the time derivative)

$$(2.3) \quad \begin{cases} \dot{\mathbf{y}} + A\mathbf{y} = \mathbf{u} & \text{in } (0, T), \\ \mathbf{y}(0) = \mathbf{y}_0, \end{cases} \quad \begin{cases} \dot{\boldsymbol{\lambda}} - A^T \boldsymbol{\lambda} = \mathbf{y} - \hat{\mathbf{y}} & \text{in } (0, T), \\ \boldsymbol{\lambda}(T) = -\gamma(\mathbf{y}(T) - \hat{\mathbf{y}}(T)), \end{cases}$$

103 where  $\boldsymbol{\lambda}(t) = \nu \mathbf{u}(t)$  for all  $t \in \Omega$ . Eliminating  $\mathbf{u}$ , we obtain in matrix form

$$(2.3) \quad \begin{cases} \begin{pmatrix} \dot{\mathbf{y}} \\ \dot{\boldsymbol{\lambda}} \end{pmatrix} + \begin{pmatrix} A & -\nu^{-1}I \\ -I & -A^T \end{pmatrix} \begin{pmatrix} \mathbf{y} \\ \boldsymbol{\lambda} \end{pmatrix} = \begin{pmatrix} 0 \\ -\hat{\mathbf{y}} \end{pmatrix} & \text{in } (0, T), \\ \mathbf{y}(0) = \mathbf{y}_0, \\ \boldsymbol{\lambda}(T) + \gamma \mathbf{y}(T) = \gamma \hat{\mathbf{y}}(T), \end{cases}$$

105 where  $I$  is the identity. If  $A$  is symmetric,  $A = A^T$ , which is natural for discretizations  
106 of  $-\Delta$ , then it can be diagonalized,  $A = PDP^{-1}$ ,  $D := \text{diag}(d_1, \dots, d_n)$  with  $d_i$  the  
107  $i$ -th eigenvalue of  $A$ . The system (2.3) can thus also be diagonalized

$$(2.3) \quad \begin{cases} \begin{pmatrix} \dot{\mathbf{z}} \\ \dot{\boldsymbol{\mu}} \end{pmatrix} + \begin{pmatrix} D & -\nu^{-1}I \\ -I & -D \end{pmatrix} \begin{pmatrix} \mathbf{z} \\ \boldsymbol{\mu} \end{pmatrix} = \begin{pmatrix} 0 \\ -\hat{\mathbf{z}} \end{pmatrix} & \text{in } (0, T), \\ \mathbf{z}(0) = \mathbf{z}_0, \\ \boldsymbol{\mu}(T) + \gamma \mathbf{z}(T) = \gamma \hat{\mathbf{z}}(T), \end{cases}$$

109 where  $\mathbf{z} := P^{-1}\mathbf{y}$ ,  $\boldsymbol{\mu} := P^{-1}\boldsymbol{\lambda}$ ,  $\hat{\mathbf{z}} := P^{-1}\hat{\mathbf{y}}$  and  $\mathbf{z}_0 := P^{-1}\mathbf{y}_0$ . This system then  
 110 represents  $n$  independent  $2 \times 2$  systems of ODEs of the form

$$111 \quad (2.4) \quad \begin{cases} \begin{pmatrix} \dot{z}_{(i)} \\ \dot{\mu}_{(i)} \end{pmatrix} + \begin{pmatrix} d_i & -\nu^{-1} \\ -1 & -d_i \end{pmatrix} \begin{pmatrix} z_{(i)} \\ \mu_{(i)} \end{pmatrix} = \begin{pmatrix} 0 \\ -\hat{z}_{(i)} \end{pmatrix} \text{ in } (0, T), \\ z_{(i)}(0) = z_{(i),0}, \\ \mu_{(i)}(T) + \gamma z_{(i)}(T) = \gamma \hat{z}_{(i)}(T), \end{cases}$$

112 where  $z_{(i)}$ ,  $\mu_{(i)}$ ,  $\hat{z}_{(i)}$  are the  $i$ -th components of the vectors  $\mathbf{z}$ ,  $\boldsymbol{\mu}$ ,  $\hat{\mathbf{z}}$ . Isolating the  
 113 variable in each equation in (2.4), we find the identities

$$114 \quad (2.5) \quad \mu_{(i)} = \nu(\dot{z}_{(i)} + d_i z_{(i)}), \quad z_{(i)} = \dot{\mu}_{(i)} - d_i \mu_{(i)} + \hat{z}_{(i)}.$$

115 We use the identity of  $z$  to eliminate  $\mu$ , and obtain a second-order ODE from (2.4),

$$116 \quad (2.6) \quad \begin{cases} \ddot{z}_{(i)} - (d_i^2 + \nu^{-1})z_{(i)} = -\nu^{-1}\hat{z}_{(i)} \text{ in } (0, T), \\ z_{(i)}(0) = z_{(i),0}, \\ \dot{z}_{(i)}(T) + (\nu^{-1}\gamma + d_i)z_{(i)}(T) = \nu^{-1}\gamma\hat{z}_{(i)}(T). \end{cases}$$

117 Similarly, we can also eliminate  $z$  to get

$$118 \quad (2.7) \quad \begin{cases} \ddot{\mu}_{(i)} - (d_i^2 + \nu^{-1})\mu_{(i)} = -\dot{\hat{z}}_{(i)} - d_i\hat{z}_{(i)} \text{ in } (0, T), \\ \dot{\mu}_{(i)}(0) - d_i\mu_{(i)}(0) = z_{(i),0} - \hat{z}_{(i)}(0), \\ \gamma\dot{\mu}_{(i)}(T) + (1 - \gamma d_i)\mu_{(i)}(T) = 0. \end{cases}$$

119 To simplify the notation in what follows, we define

$$120 \quad (2.8) \quad \sigma_i := \sqrt{d_i^2 + \nu^{-1}}, \quad \omega_i := \nu^{-1}\gamma + d_i, \quad \beta_i := 1 - \gamma d_i.$$

121 In our analysis for the error,  $\hat{\mathbf{y}}$  will equal zero, which implies  $\hat{\mathbf{z}} = 0$ , and the solution  
 122 of (2.6) and (2.7) is then

$$123 \quad (2.9) \quad z_{(i)}(t) \text{ or } \mu_{(i)}(t) = A_i \cosh(\sigma_i t) + B_i \sinh(\sigma_i t),$$

124 where  $A_i, B_i$  are two coefficients.

125 *Remark 2.1.* Our arguments above work for any diagonalizable matrix  $A$ , and  
 126 thus our results will apply to more general parabolic optimal control problems than  
 127 the heat equation. Note also that the diagonalization is only a theoretical tool for  
 128 our convergence analysis, and not needed to run our new time domain decomposition  
 129 algorithms.

130 **3. Dirichlet-Neumann and Neumann-Dirichlet algorithms in time.** We  
 131 now apply Dirichlet-Neumann (DN) and Neumann-Dirichlet (ND) techniques in time  
 132 to obtain our new time domain decomposition algorithms to solve the system (2.4),  
 133 and study their convergence. Focusing on the error equations, we set the initial  
 134 condition  $\mathbf{y}_0 = 0$  (i.e.,  $\mathbf{z}_0 = 0$ ) and the target functions  $\hat{\mathbf{y}} = 0$  (i.e.,  $\hat{\mathbf{z}} = 0$ ). We  
 135 decompose the time domain  $\Omega := (0, T)$  into two non-overlapping time subdomains  
 136  $\Omega_1 := (0, \alpha)$  and  $\Omega_2 := (\alpha, T)$ , where  $\alpha$  is the interface. We denote by  $z_{j,(i)}$  and  $\mu_{j,(i)}$   
 137 the restriction to  $\Omega_j$ ,  $j = 1, 2$  of  $z_{(i)}$  and  $\mu_{(i)}$ . Since system (2.4) is a forward-backward  
 138 system, it appears natural at first sight to keep this property for the decomposed case,  
 139 as illustrated in Figure 1: we expect to have a final condition for the adjoint state

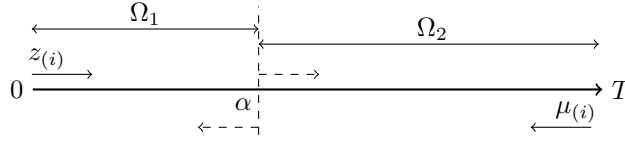


FIG. 1. Illustration of the forward-backward system.

140  $\mu_{(i)}$  in  $\Omega_1$  since we already have an initial condition for  $z_{(i)}$ ; similarly, we expect to  
 141 have an initial condition for the primal state  $z_{(i)}$  in  $\Omega_2$  since we already have a final  
 142 condition for  $\mu_{(i)}$ . Therefore, a natural DN algorithm in time solves for the iteration  
 143 index  $k = 1, 2, \dots$

$$(3.1) \quad \left\{ \begin{array}{l} \left( \begin{array}{c} \dot{z}_{1,(i)}^k \\ \dot{\mu}_{1,(i)}^k \end{array} \right) + \begin{pmatrix} d_i & -\nu^{-1} \\ -1 & -d_i \end{pmatrix} \begin{pmatrix} z_{1,(i)}^k \\ \mu_{1,(i)}^k \end{pmatrix} = \begin{pmatrix} 0 \\ 0 \end{pmatrix} \text{ in } \Omega_1, \\ z_{1,(i)}^k(0) = 0, \\ \mu_{1,(i)}^k(\alpha) = f_{\alpha,(i)}^{k-1}, \\ \left( \begin{array}{c} \dot{z}_{2,(i)}^k \\ \dot{\mu}_{2,(i)}^k \end{array} \right) + \begin{pmatrix} d_i & -\nu^{-1} \\ -1 & -d_i \end{pmatrix} \begin{pmatrix} z_{2,(i)}^k \\ \mu_{2,(i)}^k \end{pmatrix} = \begin{pmatrix} 0 \\ 0 \end{pmatrix} \text{ in } \Omega_2, \\ z_{2,(i)}^k(\alpha) = z_{1,(i)}^k(\alpha), \\ \mu_{2,(i)}^k(T) + \gamma z_{2,(i)}^k(T) = 0, \end{array} \right.$$

145 and then the transmission condition is updated by

$$(3.2) \quad f_{\alpha,(i)}^k := (1 - \theta) f_{\alpha,(i)}^{k-1} + \theta \mu_{2,(i)}^k(\alpha),$$

147 with a relaxation parameter  $\theta \in (0, 1)$ . However, there are many other ways to  
 148 decouple in time using DN and ND techniques for problem (2.4): we can apply the  
 149 technique to both states  $(z_{(i)}, \mu_{(i)})$  as in (3.1), or we can apply it just to one of these  
 150 two states in the reduced forms (2.6) and (2.7). And with the identities (2.5), we can  
 151 transfer the Dirichlet and the Neumann transmission condition from one state to the  
 152 other. We list in Table 1 all possible new time domain decomposition algorithms we  
 153 can obtain, along with their equivalent representations in terms of other formulations.  
 154 The algorithms can be classified into three main categories, and each category is  
 155 composed of two blocks, the first block represents a DN technique applied to (2.4),  
 156 whereas the second block represents a ND technique. Each block contains three  
 157 rows: the first row is the algorithm applied to formulation (2.4), the second row the  
 158 algorithm applied to formulation (2.6) and the third row the algorithm applied to  
 159 formulation (2.7).

160 *Remark 3.1.* In Table 1, the transmission conditions  $\ddot{z}_{(i)} + d_i \dot{z}_{(i)}$  and  $\ddot{\mu}_{(i)} - d_i \dot{\mu}_{(i)}$   
 161 are in fact Robin type conditions, since, using the identity (2.5) of  $z_{(i)}$  and  $\mu_{(i)}$ , we find  
 162  $\dot{z}_{(i)} = \dot{\mu}_{(i)} - d_i \dot{\mu}_{(i)}$  and  $\dot{\mu}_{(i)} = \dot{z}_{(i)} + d_i \dot{z}_{(i)}$ . On the other hand, from the first equation  
 163 of (2.6) and of (2.7), we have  $\ddot{z}_{(i)} - \sigma_i^2 z_{(i)} = 0$  and  $\ddot{\mu}_{(i)} - \sigma_i^2 \mu_{(i)} = 0$ . Substituting  
 164  $\ddot{z}_{(i)}$  and  $\ddot{\mu}_{(i)}$  gives  $\dot{\mu}_{(i)} = \ddot{z}_{(i)} + d_i \dot{z}_{(i)} = d_i \dot{z}_{(i)} + \sigma_i^2 z_{(i)}$  and  $\dot{z}_{(i)} = \dot{\mu}_{(i)} - d_i \dot{\mu}_{(i)} =$   
 165  $\sigma_i^2 \mu_{(i)} - d_i \dot{\mu}_{(i)}$ . Thus the transmission conditions containing a second derivative in  
 166 Table 1 are indeed Robin type conditions. We decided to keep the notations  $\ddot{z}_{(i)}$  and  
 167  $\ddot{\mu}_{(i)}$  in Table 1 to show the direct link between the two states  $z_{(i)}$  and  $\mu_{(i)}$ .

TABLE 1

Combinations of the DN and ND algorithms. The letter R stands for a Robin type condition.

	Problem	$\Omega_1$	$\Omega_2$	algorithm type
Category I: $(z_{(i)}, \mu_{(i)})$	(2.4)	$\mu_{(i)}$	$\dot{z}_{(i)}$	(DN)
	(2.6)	$\dot{z}_{(i)} + d_i z_{(i)}$	$\dot{z}_{(i)}$	(RN)
	(2.7)	$\mu_{(i)}$	$\ddot{\mu}_{(i)} - d_i \dot{\mu}_{(i)}$	(DR)
	(2.4)	$\dot{\mu}_{(i)}$	$z_{(i)}$	(ND)
	(2.6)	$\ddot{z}_{(i)} + d_i \dot{z}_{(i)}$	$z_{(i)}$	(RD)
	(2.7)	$\dot{\mu}_{(i)}$	$\dot{\mu}_{(i)} - d_i \mu_{(i)}$	(NR)
Category II: $z_{(i)}$	(2.4)	$z_{(i)}$	$\dot{z}_{(i)}$	(DN)
	(2.6)	$z_{(i)}$	$\dot{z}_{(i)}$	(DN)
	(2.7)	$\dot{\mu}_{(i)} - d_i \mu_{(i)}$	$\ddot{\mu}_{(i)} - d_i \dot{\mu}_{(i)}$	(RR)
	(2.4)	$\dot{z}_{(i)}$	$z_{(i)}$	(ND)
	(2.6)	$\dot{z}_{(i)}$	$z_{(i)}$	(ND)
	(2.7)	$\ddot{\mu}_{(i)} - d_i \dot{\mu}_{(i)}$	$\dot{\mu}_{(i)} - d_i \mu_{(i)}$	(RR)
Category III: $\mu_{(i)}$	(2.4)	$\mu_{(i)}$	$\dot{\mu}_{(i)}$	(DN)
	(2.6)	$\dot{z}_{(i)} + d_i z_{(i)}$	$\ddot{z}_{(i)} + d_i \dot{z}_{(i)}$	(RR)
	(2.7)	$\mu_{(i)}$	$\dot{\mu}_{(i)}$	(DN)
	(2.4)	$\dot{\mu}_{(i)}$	$\mu_{(i)}$	(ND)
	(2.6)	$\ddot{z}_{(i)} + d_i \dot{z}_{(i)}$	$\dot{z}_{(i)} + d_i z_{(i)}$	(RR)
	(2.7)	$\dot{\mu}_{(i)}$	$\mu_{(i)}$	(ND)

168 However, there are other interpretations of some transmission conditions in certain  
 169 circumstances. For instance, let us take the Neumann condition  $\dot{z}_{(i)}$  in the second  
 170 block of Category II for the problem (2.4), it can also be interpreted as a Robin  
 171 condition  $\sigma_i^2 \mu_{(i)} - d_i \dot{\mu}_{(i)}$  using the above argument. Then, this algorithm can also  
 172 be read as a Robin-Dirichlet (RD) type algorithm instead of a Neumann-Dirichlet  
 173 type. Moreover, this interpretation is particularly useful in this case, since it reveals  
 174 the fact that the forward-backward property of the problem (2.4) is still kept by this  
 175 algorithm. Otherwise, we can also use the identity of  $\mu_{(i)}$  in (2.5) to transfer this  
 176 Neumann condition  $\dot{z}_{(i)}$  to  $\mu_{(i)} - d_i z_{(i)}$ . This is also useful from a numerical point of  
 177 view, since we can transfer a Neumann condition to a Dirichlet type condition. This  
 178 will be used in detail in the following analysis.

179 **3.1. Category I.** We start with the algorithms in Category I, which run on the  
 180 pair  $(z_{(i)}, \mu_{(i)})$  to solve (2.4), and study the DN and then the ND variant.

181 **3.1.1. Dirichlet-Neumann algorithm (DN<sub>1</sub>).** This is (3.1), at first sight the  
 182 most natural method that keeps the forward-backward structure as in the original  
 183 problem (2.4). To analyze the convergence behavior, we can choose any of the prob-  
 184 lem formulations (2.6), (2.7), since they are equivalent to (2.4). Choosing (2.6), the  
 185 algorithm DN<sub>1</sub> for  $i = 1, \dots, n$ , and iteration  $k = 1, 2, \dots$  is given by

$$186 \quad (3.3) \quad \begin{cases} \dot{z}_{1,(i)}^k - \sigma_i^2 z_{1,(i)}^k = 0 \text{ in } \Omega_1, \\ z_{1,(i)}^k(0) = 0, \\ \dot{z}_{1,(i)}^k(\alpha) + d_i z_{1,(i)}^k(\alpha) = f_{\alpha,(i)}^{k-1}, \end{cases} \quad \begin{cases} \dot{z}_{2,(i)}^k - \sigma_i^2 z_{2,(i)}^k = 0 \text{ in } \Omega_2, \\ \dot{z}_{2,(i)}^k(\alpha) = \dot{z}_{1,(i)}^k(\alpha), \\ \dot{z}_{2,(i)}^k(T) + \omega_i z_{2,(i)}^k(T) = 0, \end{cases}$$

187 and the update of the transmission condition defined in (3.2) becomes

$$188 \quad (3.4) \quad f_{\alpha,(i)}^k = (1 - \theta) f_{\alpha,(i)}^{k-1} + \theta (\dot{z}_{2,(i)}^k(\alpha) + d_i z_{2,(i)}^k(\alpha)).$$

189 This is a Robin-Neumann type algorithm applied to solve the problem (2.6). Using  
190 the general solution (2.9), and the initial and final condition, we find

$$191 \quad (3.5) \quad z_{1,(i)}^k(t) = A_i^k \sinh(\sigma_i t), \quad z_{2,(i)}^k(t) = B_i^k \left( \sigma_i \cosh(\sigma_i(T-t)) + \omega_i \sinh(\sigma_i(T-t)) \right),$$

192 where  $A_i^k$  and  $B_i^k$  are determined by the transmission conditions at  $\alpha$  in (3.3). Note  
193 that we will use (3.5) in the analysis for all algorithms, since only the transmission con-  
194 ditions will change. Inserting (3.5) at the interface  $\alpha$  into (3.3) and solving for  $A_i^k$ ,  $B_i^k$

195 gives  $A_i^k = \frac{f_{\alpha,(i)}^{k-1}}{\sigma_i \cosh(a_i) + d_i \sinh(a_i)}$  and  $B_i^k = \frac{-f_{\alpha,(i)}^{k-1} \cosh(a_i)}{(\sigma_i \cosh(a_i) + d_i \sinh(a_i))(\sigma_i \sinh(b_i) + \omega_i \cosh(b_i))}$ ,  
196 where we let  $a_i := \sigma_i \alpha$  and  $b_i := \sigma_i(T - \alpha)$  to simplify the notations, and  $a_i + b_i = \sigma_i T$ .  
197 Using the update of the transmission condition (3.4), we obtain  $f_{\alpha,(i)}^k = (1 - \theta) f_{\alpha,(i)}^{k-1} +$   
198  $\theta f_{\alpha,(i)}^{k-1} \nu^{-1} \frac{\sigma_i \gamma + \beta_i \tanh(b_i)}{(\sigma_i + d_i \tanh(a_i))(\omega_i + \sigma_i \tanh(b_i))}$ , which leads to the following result.

199 **THEOREM 3.2.** *The algorithm  $DN_1$  (3.1)-(3.2) converges if and only if*

$$200 \quad (3.6) \quad \rho_{DN_1} := \max_{d_i \in \lambda(A)} \left| 1 - \theta \left( 1 - \nu^{-1} \frac{\sigma_i \gamma + \beta_i \tanh(b_i)}{(\sigma_i + d_i \tanh(a_i))(\omega_i + \sigma_i \tanh(b_i))} \right) \right| < 1,$$

201 where  $\lambda(A)$  is the spectrum of the matrix  $A$ .

202 *Remark 3.3.* Instead of focusing on the state  $z_{(i)}$  for the analysis, we could also  
203 have focused on the state  $\mu_{(i)}$ , which gives the same result, see Appendix A.

204 To get more insight in the convergence behavior, we consider a few special cases.

205 **COROLLARY 3.4.** *If the matrix  $A$  is not singular, then the algorithm  $DN_1$  (3.1)-*  
206 *(3.2) for  $\theta = 1$  converges for all initial guesses.*

207 *Proof.* Substituting  $\theta = 1$  into (3.6), we have

$$208 \quad (3.7) \quad \rho_{DN_1}|_{\theta=1} = \nu^{-1} \max_{d_i \in \lambda(A)} \left| \frac{\sigma_i \gamma + \beta_i \tanh(b_i)}{(\sigma_i + d_i \tanh(a_i))(\omega_i + \sigma_i \tanh(b_i))} \right|.$$

209 Using the definition of  $\sigma_i$ ,  $\beta_i$  and  $\omega_i$  from (2.8), the numerator can be written as  $\sigma_i \gamma +$   
210  $\beta_i \tanh(b_i) = \gamma(\sigma_i - d_i \tanh(b_i)) + \tanh(b_i)$ . Since  $0 < \tanh(x) < 1, \forall x > 0$  and  $\sigma_i -$   
211  $d_i \tanh(b_i) > 0$ , both the numerator and the denominator in (3.7) are positive. Now  
212 the difference between the numerator and the denominator is  $(\sigma_i + d_i \tanh(a_i))(\omega_i +$   
213  $\sigma_i \tanh(b_i)) - \nu^{-1}(\sigma_i \gamma + \beta_i \tanh(b_i)) = (1 + \tanh(b_i) \tanh(a_i))(\sigma_i d_i + \omega_i d_i \tanh(\sigma_i T)) >$   
214  $0$ , meaning that for each eigenvalue  $d_i$ ,  $0 < \nu^{-1} \frac{\sigma_i \gamma + \beta_i \tanh(b_i)}{(\sigma_i + d_i \tanh(a_i))(\omega_i + \sigma_i \tanh(b_i))} < 1$ .  $\square$

215 *Remark 3.5.* For the Laplace operator with homogeneous Dirichlet boundary con-  
216 ditions in our model problem (1.2), there is no zero eigenvalue for its discretization  
217 matrix  $A$ . If an eigenvalue  $d_i = 0$ , we have  $\sigma_i|_{d_i=0} = \sqrt{\nu^{-1}}$ ,  $\omega_i|_{d_i=0} = \gamma \nu^{-1}$  and  
218  $\beta_i|_{d_i=0} = 1$ . Substituting these values into the convergence factor (3.7), we find  
219  $\rho_{DN_1}|_{\theta=1, d_i=0} = \nu^{-1} \frac{\sqrt{\nu^{-1}} \gamma + \tanh(\sqrt{\nu^{-1}}(T - \alpha))}{\sqrt{\nu^{-1}}(\gamma \nu^{-1} + \sqrt{\nu^{-1}} \tanh(\sqrt{\nu^{-1}}(T - \alpha)))} = 1$ , and convergence is lost.  
220 The convergence behavior of the algorithm  $DN_1$  for small eigenvalues is thus not  
221 good. Furthermore, inserting  $d_i = 0$  into (3.6) and using the above result, we find  
222 that  $\rho_{DN_1}|_{d_i=0} = 1$ , independently of the relaxation parameter  $\theta$  and the interface  
223 position  $\alpha$ : relaxation can not fix this problem.

224 *Remark 3.6.* If some  $d_i$  goes to infinity, we have  $\sigma_i \sim_\infty d_i$  and  $\omega_i \sim_\infty d_i$ , and  
225 therefore  $\lim_{d_i \rightarrow \infty} \left| 1 - \theta \left( 1 - \nu^{-1} \frac{\sigma_i \gamma + \beta_i \tanh(b_i)}{(\sigma_i + d_i \tanh(a_i))(\omega_i + \sigma_i \tanh(b_i))} \right) \right| = |1 - \theta|$ , which is  
226 independent of  $\alpha$ , so high frequency convergence is robust with relaxation. One can  
227 use  $\theta = 1$  to get a good smoother, with the following convergence factor estimate.

228 COROLLARY 3.7. *If  $A$  is positive semi-definite, then the algorithm  $DN_1$  (3.1)-*  
 229 *(3.2) with  $\theta = 1$  satisfies the convergence estimate  $\rho_{DN_1}|_{\theta=1} \leq \frac{1+\gamma\sigma_{\min}}{\nu d_{\min}^2}$ , with  $d_{\min} :=$*   
 230  *$\min \lambda(A)$  the smallest eigenvalue of  $A$ .*

231 *Proof.* Since for  $\theta = 1$ , Corollary 3.4 shows that the convergence factor is between  
 232 0 and 1 for each eigenvalue  $d_i$ , we can take (3.7) and remove the absolute value,  
 233  $\rho_{DN_1}|_{\theta=1} = \nu^{-1} \max_{d_i \in \lambda(A)} \frac{\tanh(b_i) + \gamma(\sigma_i - d_i \tanh(b_i))}{(\sigma_i + d_i \tanh(a_i))(\omega_i + \sigma_i \tanh(b_i))}$ . Using the definition of  $\sigma_i$   
 234 and  $\omega_i$  from (2.8), we have  $\sigma_i > d_i \geq 0$  and  $\omega_i \geq d_i \geq 0$ . Since  $0 < \tanh(x) < 1, \forall x >$   
 235 0, we obtain that  $\sigma_i + d_i \tanh(a_i) \geq d_i$ ,  $\omega_i + \sigma_i \tanh(b_i) \geq d_i$  and  $\sigma_i - d_i \tanh(b_i) \leq \sigma_i$ .  
 236 This implies  $\frac{\tanh(b_i) + \gamma(\sigma_i - d_i \tanh(b_i))}{(\sigma_i + d_i \tanh(a_i))(\omega_i + \sigma_i \tanh(b_i))} \leq \frac{1 + \gamma\sigma_i}{d_i^2} = \frac{1}{d_i} \left( \frac{1}{d_i} + \gamma \frac{\sigma_i}{d_i} \right)$ . Using once again  
 237 the definition of  $\sigma_i$  from (2.8), we find  $\frac{\sigma_i}{d_i} = \sqrt{1 + \frac{\nu^{-1}}{d_i^2}} \leq \sqrt{1 + \frac{\nu^{-1}}{d_{\min}^2}}$ . Hence, we have  
 238  $\frac{1 + \gamma\sigma_i}{d_i^2} \leq \frac{1 + \gamma\sigma_{\min}}{d_{\min}^2}$ , which concludes the proof.  $\square$

239 Since  $A$  comes from a spatial discretization, the smallest eigenvalue of  $A$  depends only  
 240 little on the spatial mesh size, and convergence is thus robust under mesh refinement.  
 241 Corollary 3.7 is however less useful when  $\nu$  is small: for example for  $\gamma = 0$ , the bound  
 242 is less than one only if  $\nu > \frac{1}{d_{\min}^2}$ , but we have also the following convergence result.

243 THEOREM 3.8. *The algorithm  $DN_1$  (3.1)-(3.2) converges for all initial guesses*  
 244 *under the assumption that the matrix  $A$  is not singular.*

245 *Proof.* From Corollary 3.4, we know that the convergence factor satisfies  $0 <$   
 246  $\rho_{DN_1}|_{\theta=1} < 1$ . Using its definition (3.6), we find for  $\theta \in (0, 1)$ ,  $0 < 1 - \theta < \rho_{DN_1} =$   
 247  $1 - \theta(1 - \rho_{DN_1}|_{\theta=1}) < 1$ , which concludes the proof.  $\square$

248 *Remark 3.9.* As shown in the previous proof, the function  $g(\theta) := 1 - \theta(1 -$   
 249  $\rho_{DN_1}|_{\theta=1})$  is decreasing for  $\theta \in (0, 1)$ , which makes  $\theta = 1$  the best relaxation param-  
 250 eter. This is further confirmed by our numerical experiments (see Figure 4). Due  
 251 to the bad convergence behavior of the algorithm  $DN_1$  for small eigenvalues, it only  
 252 makes this most natural DN algorithm a good smoother but not a good solver.

253 **3.1.2. Neumann-Dirichlet algorithm ( $ND_1$ ).** We now invert the two condi-  
 254 tions, and apply the Neumann condition to the state  $\mu_{(i)}$  in  $\Omega_1$  and the Dirichlet  
 255 condition to the state  $z_{(i)}$  in  $\Omega_2$ , still respecting the forward-backward structure. For  
 256 iteration index  $k = 1, 2, \dots$ , the algorithm  $ND_1$  computes

$$\begin{aligned}
 & \left\{ \begin{array}{l} \left( \begin{array}{c} z_{1,(i)}^k \\ \mu_{1,(i)}^k \end{array} \right) + \begin{pmatrix} d_i & -\nu^{-1} \\ -1 & -d_i \end{pmatrix} \left( \begin{array}{c} z_{1,(i)}^k \\ \mu_{1,(i)}^k \end{array} \right) = \begin{pmatrix} 0 \\ 0 \end{pmatrix} \text{ in } \Omega_1, \\ z_{1,(i)}^k(0) = 0, \\ \mu_{1,(i)}^k(\alpha) = \mu_{2,(i)}^k(\alpha), \end{array} \right. \\
 257 \quad (3.8) \quad & \left\{ \begin{array}{l} \left( \begin{array}{c} z_{2,(i)}^k \\ \mu_{2,(i)}^k \end{array} \right) + \begin{pmatrix} d_i & -\nu^{-1} \\ -1 & -d_i \end{pmatrix} \left( \begin{array}{c} z_{2,(i)}^k \\ \mu_{2,(i)}^k \end{array} \right) = \begin{pmatrix} 0 \\ 0 \end{pmatrix} \text{ in } \Omega_2, \\ z_{2,(i)}^k(\alpha) = f_{\alpha,(i)}^{k-1}, \\ \mu_{2,(i)}^k(T) + \gamma z_{2,(i)}^k(T) = 0, \end{array} \right.
 \end{aligned}$$

258 and we update the transmission condition by

$$259 \quad (3.9) \quad f_{\alpha,(i)}^k := (1 - \theta) f_{\alpha,(i)}^{k-1} + \theta z_{1,(i)}^k(\alpha), \quad \theta \in (0, 1).$$



260 For the convergence analysis, we choose to use the formulation (2.7), i.e.

$$261 \quad (3.10) \quad \begin{cases} \ddot{\mu}_{1,(i)}^k - \sigma_i^2 \mu_{1,(i)}^k = 0 \text{ in } \Omega_1, \\ \dot{\mu}_{(i)}^k(0) - d_i \mu_{(i)}^k(0) = 0, \\ \dot{\mu}_{1,(i)}^k(\alpha) = \dot{\mu}_{2,(i)}^k(\alpha), \end{cases} \quad \begin{cases} \ddot{\mu}_{2,(i)}^k - \sigma_i^2 \mu_{2,(i)}^k = 0 \text{ in } \Omega_2, \\ \dot{\mu}_{2,(i)}^k(\alpha) - d_i \mu_{2,(i)}^k(\alpha) = f_{\alpha,(i)}^{k-1}, \\ \gamma \dot{\mu}_{(i)}^k(T) + \beta_i \mu_{(i)}^k(T) = 0, \end{cases}$$

262 where the update of the transmission condition (3.9) becomes

$$263 \quad (3.11) \quad f_{\alpha,(i)}^k = (1 - \theta) f_{\alpha,(i)}^{k-1} + \theta (\dot{\mu}_{1,(i)}^k(\alpha) - d_i \mu_{1,(i)}^k(\alpha)), \quad \theta \in (0, 1).$$

264 The algorithm ND<sub>1</sub> (3.8) can thus be interpreted as a NR type algorithm (3.10).

265 Using the general solution (2.9) and the initial and final conditions, we get

$$266 \quad (3.12) \quad \begin{aligned} \mu_{1,(i)}^k(t) &= A_i^k (\sigma_i \cosh(\sigma_i t) + d_i \sinh(\sigma_i t)), \\ \mu_{2,(i)}^k(t) &= B_i^k (\gamma \sigma_i \cosh(\sigma_i(T-t)) + \beta_i \sinh(\sigma_i(T-t))), \end{aligned}$$

267 and from the transmission condition in (3.10) on each domain, and we obtain  $A_i^k =$

$$268 \quad \frac{f_{\alpha,(i)}^{k-1} (\sigma_i \gamma \sinh(b_i) + \beta_i \cosh(b_i))}{(\omega_i \sinh(b_i) + \sigma_i \cosh(b_i)) (\sigma_i \sinh(a_i) + d_i \cosh(a_i))} \quad \text{and} \quad B_i^k = \frac{-f_{\alpha,(i)}^{k-1}}{\omega_i \sinh(b_i) + \sigma_i \cosh(b_i)}.$$

269 Using the relation (3.11), we find  $f_{\alpha,(i)}^{k-1} = (1 - \theta) f_{\alpha,(i)}^{k-1} + \theta f_{\alpha,(i)}^{k-1} \nu^{-1} \frac{\sigma_i \gamma + \beta_i \coth(b_i)}{(\sigma_i + d_i \coth(a_i)) (\omega_i + \sigma_i \coth(b_i))}$ ,

270 which leads to the following result.

271 **THEOREM 3.10.** *The algorithm ND<sub>1</sub> (3.8)-(3.9) converges if and only if*

$$272 \quad (3.13) \quad \rho_{ND_1} := \max_{d_i \in \lambda(A)} \left| 1 - \theta \left( 1 - \nu^{-1} \frac{\sigma_i \gamma + \beta_i \coth(b_i)}{(\sigma_i + d_i \coth(a_i)) (\omega_i + \sigma_i \coth(b_i))} \right) \right| < 1.$$

273 The convergence factor of the algorithm ND<sub>1</sub> (3.13) is very similar to that of DN<sub>1</sub> (3.6).

274 For instance, the behavior for large and small eigenvalues shown in Remarks 3.5 and

275 3.6 still hold: when inserting  $d_i = 0$  into (3.13) we find  $\rho_{ND_1}|_{d_i=0} = |1 - \theta(1 -$

$$276 \quad \nu^{-1} \frac{\sqrt{\nu^{-1} \gamma + \coth(\sqrt{\nu^{-1}(T-\alpha))}}{\sqrt{\nu^{-1}(\gamma \nu^{-1} + \sqrt{\nu^{-1} \coth(\sqrt{\nu^{-1}(T-\alpha))})}})| = 1,$$

277 again independent of the relaxation parameter  $\theta$  and the interface position  $\alpha$ ; and when the eigenvalue  $d_i$  goes to infinity, we

278 find  $\lim_{d_i \rightarrow \infty} |1 - \theta(1 - \nu^{-1} \frac{\sigma_i \gamma + \beta_i \coth(b_i)}{(\sigma_i + d_i \coth(a_i)) (\omega_i + \sigma_i \coth(b_i))})| = |1 - \theta|$ , again independent

279 of the interface position  $\alpha$ . Due however to the presence of the hyperbolic cotangent

280 function in (3.13) instead of the hyperbolic tangent function in (3.6), we need further

281 assumptions to obtain results like Corollaries 3.4 and 3.7. Indeed, substituting  $\theta = 1$

282 into (3.13) and using the definition of  $\sigma_i, \beta_i$  from (2.8), the numerator reads  $\sigma_i \gamma +$

283  $\beta_i \coth(b_i) = \gamma(\sqrt{d_i^2 + \nu^{-1}} - d_i \coth(\sqrt{d_i^2 + \nu^{-1}(T-\alpha)})) + \coth(\sqrt{d_i^2 + \nu^{-1}(T-\alpha)})$ .

284 Depending on  $\gamma, \nu$  and  $\alpha$ , this value could be negative. However, by setting  $\gamma = 0$ ,

285 the numerator is guaranteed to be positive, and we obtain the following results.

286 **COROLLARY 3.11.** *If  $A$  is not singular and the parameter  $\gamma = 0$ , then the algo-*

287 *rithm ND<sub>1</sub> (3.8)-(3.9) for  $\theta = 1$  converges for all initial guesses.*

288 *Proof.* Substituting  $\theta = 1$  and  $\gamma = 0$  into (3.13), we get

$$289 \quad (3.14) \quad \rho_{ND_2}|_{\theta=1} = \nu^{-1} \max_{d_i \in \lambda(A)} \left| \frac{\coth(b_i)}{(\sigma_i + d_i \coth(a_i)) (d_i + \sigma_i \coth(b_i))} \right|.$$

290 Since  $\coth(x) > 1, \forall x > 0$ , both the numerator and the denominator in (3.14) are

291 positive, and the difference between them is  $(\sigma_i + d_i \coth(a_i)) (d_i + \sigma_i \coth(b_i)) -$

292  $\nu^{-1} \coth(b_i) = (\coth(a_i) + \coth(b_i)) (d_i^2 + \sigma_i d_i \coth(\sigma_i T)) > 0$ , meaning that for each

293 eigenvalue  $d_i, 0 < \nu^{-1} \frac{\coth(b_i)}{(\sigma_i + d_i \coth(a_i)) (\omega_i + \sigma_i \coth(b_i))} < 1$ , which concludes the proof.  $\square$

294 COROLLARY 3.12. *If  $A$  is positive semi-definite and the parameter  $\gamma = 0$ , then*  
 295 *the algorithm  $ND_1$  (3.8)-(3.9) for  $\theta = 1$  satisfies the convergence estimate*

$$296 \quad (3.15) \quad \rho_{ND_1}|_{\theta=1} \leq \frac{\coth(\sigma_{\min}(T - \alpha))}{\nu(\sigma_{\min} + d_{\min})^2}.$$

297 *Proof.* Since we have shown in Corollary 3.11 that the convergence factor is be-  
 298 tween 0 and 1 for each eigenvalue  $d_i$ , we can take (3.14) and remove the absolute value,  
 299  $\rho_{ND_2}|_{\theta=1} = \nu^{-1} \max_{d_i \in \lambda(A)} \frac{\coth(b_i)}{(\sigma_i + d_i \coth(a_i))(d_i + \sigma_i \coth(b_i))}$ . Since  $\sigma_i = \sqrt{d_i^2 + \nu^{-1}} \geq$   
 300  $d_i \geq 0$  and  $\coth(x) > 1, \forall x > 0$ , we obtain that  $\sigma_i + d_i \coth(a_i) \geq \sigma_i + d_i$  and  
 301  $d_i + \sigma_i \coth(b_i) \geq \sigma_i + d_i$ . This implies that  $\frac{\coth(b_i)}{(\sigma_i + d_i \coth(a_i))(d_i + \sigma_i \coth(b_i))} \leq \frac{\coth(b_i)}{(\sigma_i + d_i)^2}$ .  
 302 Recalling  $\coth(b_i) = \coth(\sigma_i(T - \alpha))$ , and using the fact that  $d_i \geq d_{\min}$  and  $\sigma_i \geq$   
 303  $\sigma_{\min} := \sqrt{d_{\min}^2 + \nu^{-1}}$ , we find  $\frac{\coth(b_i)}{(\sigma_i + d_i)^2} \leq \frac{\coth(\sigma_{\min}(T - \alpha))}{(\sigma_{\min} + d_{\min})^2}$ , which concludes the proof.  $\square$

304 Like for  $DN_1$ , the estimate (3.15) is independent of the spatial mesh size, and since for  
 305  $\gamma = 0$ , the convergence factor satisfies  $0 < \rho_{ND_1}|_{\theta=1} < 1$  as shown in Corollary 3.11,  
 306 using the definition of the convergence factor (3.13), we obtain the following result.

307 THEOREM 3.13. *The algorithm  $ND_1$  (3.8)-(3.9) converges for all initial guesses if*  
 308  *$\gamma = 0$  and the matrix  $A$  is not singular.*

309 **3.2. Category II.** We now study algorithms in Category II which run only on  
 310 the state  $z_{(i)}$  to solve the problem (2.4), based on DN and ND techniques.

311 **3.2.1. Dirichlet-Neumann algorithm ( $DN_2$ ).** As explained in Table 1, we  
 312 apply the Dirichlet condition in  $\Omega_1$  and the Neumann condition in  $\Omega_2$  both on the  
 313 primal state  $z_{(i)}$ . For the iteration index  $k = 1, 2, \dots$ , the algorithm  $DN_2$  solves

$$314 \quad (3.16) \quad \left\{ \begin{array}{l} \left( \begin{array}{c} \dot{z}_{1,(i)}^k \\ \dot{\mu}_{1,(i)}^k \end{array} \right) + \begin{pmatrix} d_i & -\nu^{-1} \\ -1 & -d_i \end{pmatrix} \left( \begin{array}{c} z_{1,(i)}^k \\ \mu_{1,(i)}^k \end{array} \right) = \begin{pmatrix} 0 \\ 0 \end{pmatrix} \text{ in } \Omega_1, \\ z_{1,(i)}^k(0) = 0, \\ z_{1,(i)}^k(\alpha) = f_{\alpha,(i)}^{k-1}, \\ \left( \begin{array}{c} \dot{z}_{2,(i)}^k \\ \dot{\mu}_{2,(i)}^k \end{array} \right) + \begin{pmatrix} d_i & -\nu^{-1} \\ -1 & -d_i \end{pmatrix} \left( \begin{array}{c} z_{2,(i)}^k \\ \mu_{2,(i)}^k \end{array} \right) = \begin{pmatrix} 0 \\ 0 \end{pmatrix} \text{ in } \Omega_2, \\ \dot{z}_{2,(i)}^k(\alpha) = \dot{z}_{1,(i)}^k(\alpha), \\ \mu_{2,(i)}^k(T) + \gamma z_{2,(i)}^k(T) = 0, \end{array} \right.$$

315 and we update the transmission condition by

$$316 \quad (3.17) \quad f_{\alpha,(i)}^k := (1 - \theta) f_{\alpha,(i)}^{k-1} + \theta z_{2,(i)}^k(\alpha), \quad \theta \in (0, 1).$$

317 At first glance, this algorithm does not have the forward-backward structure, with  
 318 both an initial and a final condition on  $z_{1,(i)}$  in  $\Omega_1$  and nothing on  $\mu_{1,(i)}$ . However, as  
 319 mentioned in Remark 3.1, this is only a matter of interpretation: using the identity  
 320 of  $z_{(i)}$  from (2.5), we can rewrite the transmission condition  $z_{1,(i)}^k(\alpha) = f_{\alpha,(i)}^{k-1}$  as  
 321  $\dot{\mu}_{1,(i)}^k(\alpha) - d_i \mu_{1,(i)}^k(\alpha) = f_{\alpha,(i)}^{k-1}$ , and define the update (3.17) as  $f_{\alpha,(i)}^k := (1 - \theta) f_{\alpha,(i)}^{k-1} +$   
 322  $\theta(\dot{\mu}_{2,(i)}^k(\alpha) - d_i \mu_{2,(i)}^k(\alpha))$ , to rediscover the forward-backward structure. Moreover,  
 323 with the interpretation of  $\mu_{1,(i)}^k$ , the algorithm  $DN_2$  (3.16) is a RN type algorithm.

324 For the analysis, we choose the state  $z_{(i)}$  formulation: for  $i = 1, \dots, n$  and iteration  
 325 index  $k = 1, 2, \dots$ , the equivalent algorithm reads

$$326 \quad (3.18) \quad \begin{cases} \dot{z}_{1,(i)}^k - \sigma_i^2 z_{1,(i)}^k = 0 \text{ in } \Omega_1, \\ z_{1,(i)}^k(0) = 0, \\ z_{1,(i)}^k(\alpha) = f_{\alpha,(i)}^{k-1}, \end{cases} \quad \begin{cases} \dot{z}_{2,(i)}^k - \sigma_i^2 z_{2,(i)}^k = 0 \text{ in } \Omega_2, \\ z_{2,(i)}^k(\alpha) = z_{1,(i)}^k(\alpha), \\ \dot{z}_{2,(i)}^k(T) + \omega_i z_{2,(i)}^k(T) = 0, \end{cases}$$

327 where we still update the transmission condition by (3.17). Note that (3.18) is still a  
 328 DN type algorithm, like (3.16). Using the solutions (3.5) to determine the two coef-  
 329 ficients  $A_i^k$  and  $B_i^k$ , we get from (3.18)  $A_i^k = \frac{f_{\alpha,(i)}^{k-1}}{\sinh(a_i)}$  and  $B_i^k = -\frac{f_{\alpha,(i)}^{k-1} \coth(a_i)}{\sigma_i \sinh(b_i) + \omega_i \cosh(b_i)}$ .  
 330 With (3.17), we find  $f_{\alpha,(i)}^k = (1 - \theta) f_{\alpha,(i)}^{k-1} - \theta f_{\alpha,(i)}^{k-1} \coth(a_i) \frac{\sigma_i \cosh(b_i) + \omega_i \sinh(b_i)}{\sigma_i \sinh(b_i) + \omega_i \cosh(b_i)}$ , and  
 331 thus obtain the following convergence results.

332 **THEOREM 3.14.** *The algorithm  $DN_2$  (3.16)-(3.17) converges if and only if*

$$333 \quad (3.19) \quad \rho_{DN_2} := \max_{d_i \in \lambda(A)} \left| 1 - \theta \left( 1 + \coth(a_i) \frac{\sigma_i \coth(b_i) + \omega_i}{\sigma_i + \omega_i \coth(b_i)} \right) \right| < 1.$$

334 **COROLLARY 3.15.** *The algorithm  $DN_2$  for  $\theta = 1$  does not converge if  $\alpha \leq \frac{T}{2}$ .*

335 *Proof.* Substituting  $\theta = 1$  into (3.19), we have

$$336 \quad (3.20) \quad \rho_{DN_2}|_{\theta=1} = \max_{d_i \in \lambda(A)} \left| \coth(a_i) \frac{\sigma_i \coth(b_i) + \omega_i}{\sigma_i + \omega_i \coth(b_i)} \right|.$$

337 Since  $\coth(x) > 1, \forall x > 0$ , both the numerator and the denominator in (3.20) are  
 338 positive. When  $a_i \leq b_i$  (i.e.,  $\alpha \leq T - \alpha$ ), we have  $\coth(a_i) \geq \coth(b_i)$ , and thus the  
 339 difference between the numerator and the denominator is  $\coth(a_i)(\omega_i + \sigma_i \coth(b_i)) -$   
 340  $(\sigma_i + \omega_i \coth(b_i)) = \omega_i(\coth(a_i) - \coth(b_i)) + \sigma_i(\coth(b_i) \coth(a_i) - 1) > 0$ , meaning  
 341 that  $\coth(a_i) \frac{\sigma_i \coth(b_i) + \omega_i}{\sigma_i + \omega_i \coth(b_i)} > 1$ , which concludes the proof.  $\square$

342 We need some extra assumptions to conclude for the case  $\alpha > \frac{T}{2}$ .

343 **COROLLARY 3.16.** *The algorithm  $DN_2$  for  $\theta = 1$  does not converge if  $\gamma = 0$ .*

344 *Proof.* We showed in Corollary 3.15 the result for  $\alpha \leq \frac{T}{2}$ . Now  $\alpha > \frac{T}{2}$  implies that  
 345  $a_i > b_i$ , thus  $\coth(a_i) < \coth(b_i)$ . Inserting  $\gamma = 0$  into (3.20) and using the definition  
 346 of  $\sigma_i$  from (2.8), the difference between the numerator and the denominator of (3.20)  
 347 becomes  $\coth(a_i)(d_i + \sigma_i \coth(b_i)) - (\sigma_i + d_i \coth(b_i)) = (\coth(a_i) - \coth(b_i))(d_i +$   
 348  $\sigma_i \coth(b_i - a_i)) > 0$ , where we use the fact that  $d_i + \sigma_i \coth(b_i - a_i) < d_i - \sigma_i < 0$ .  
 349 This shows that  $DN_2$  for  $\theta = 1$  also does not converge for  $\alpha > \frac{T}{2}$  when  $\gamma = 0$ .  $\square$

350 Unlike in Corollary 3.7 where we have an estimate of the convergence factor for  
 351  $DN_1$ , we cannot provide a general convergence estimate for the algorithm  $DN_2$  (3.16)-  
 352 (3.17), since we showed in Corollary 3.15 and Corollary 3.16 that it does not converge  
 353 in some cases. However, we can still show the convergence behavior for extreme  
 354 eigenvalues. In particular, if the eigenvalue  $d_i = 0$ , we find

$$355 \quad (3.21) \quad \rho_{DN_2}|_{d_i=0} = \left| 1 - \theta \left( 1 + \coth(\sqrt{\nu^{-1}}\alpha) \frac{\coth(\sqrt{\nu^{-1}}(T-\alpha) + \gamma\sqrt{\nu^{-1}})}{1 + \gamma\sqrt{\nu^{-1}} \coth(\sqrt{\nu^{-1}}(T-\alpha))} \right) \right|.$$

356 When the eigenvalue goes to infinity, using Remark 3.6, we obtain  $\lim_{d_i \rightarrow \infty} \rho_{DN_2} =$   
 357  $|1 - 2\theta|$ . By equioscillating the convergence factor for small (i.e.,  $\rho_{DN_2}|_{d_i=0}$ ) and large

358 eigenvalues (i.e.,  $\rho_{\text{DN}_2}|_{d_i \rightarrow \infty}$ ), we obtain after some computations

$$359 \quad (3.22) \quad \theta_{\text{DN}_2}^* = \frac{2}{3 + \coth(\sqrt{\nu^{-1}}\alpha) \frac{\coth(\sqrt{\nu^{-1}}(T-\alpha)) + \gamma\sqrt{\nu^{-1}}}{1 + \gamma\sqrt{\nu^{-1}} \coth(\sqrt{\nu^{-1}}(T-\alpha))}}.$$

360 **THEOREM 3.17.** *If we assume that the eigenvalues of  $A$  are anywhere in the inter-*  
 361 *val  $[0, \infty)$ , then the optimal relaxation parameter  $\theta_{\text{DN}_2}^*$  for the algorithm  $\text{DN}_2$  (3.16)-*  
 362 *(3.17) with  $\gamma = 0$  is given by (3.22) and satisfies  $\theta_{\text{DN}_2}^* < \frac{1}{2}$ .*

363 *Proof.* Taking the derivative of the convergence factor  $\rho_{\text{DN}_2}$  from (3.19) with  
 364 respect to the eigenvalue  $d_i$ , we get  $\frac{d\rho_{\text{DN}_2}}{dd_i} = -\frac{d_i\alpha}{\sigma_i \sinh^2(a_i)} \frac{\sigma_i \coth(b_i) + \omega_i}{\sigma_i + \omega_i \coth(b_i)} - \frac{\nu^{-1} \coth(a_i)}{\sigma_i}$   
 365  $\frac{\beta_i(\coth^2(b_i) - 1) + \frac{d_i(T-\alpha)}{\sinh^2(b_i)}(1 - \gamma^2\nu^{-1} - 2d_i\gamma)}{(\sigma_i + \omega_i \coth(b_i))^2}$ , where we used  $\sigma_i, \omega_i$  and  $\beta_i$  from (2.8). The de-  
 366 rivative becomes negative with  $\gamma = 0$ , meaning that the convergence factor decreases  
 367 with respect to the eigenvalue  $d_i$ . We can then deduce the optimal relaxation pa-  
 368 rameter using equioscillation: inserting  $\gamma = 0$  into (3.22), the denominator becomes  
 369  $3 + \coth(\sqrt{\nu^{-1}}\alpha) \coth(\sqrt{\nu^{-1}}(T - \alpha)) < 4$ .  $\square$

370 For  $\gamma > 0$ , it is not clear when the convergence factor  $\rho_{\text{DN}_2}$  is monotonic with  
 371 respect to the eigenvalues, and thus the optimal relaxation parameter  $\theta_{\text{DN}_2}^*$  could  
 372 differ from (3.22).

373 **3.2.2. Neumann-Dirichlet algorithm (ND<sub>2</sub>).** We now invert the two condi-  
 374 tions: for the iteration index  $k = 1, 2, \dots$ , the algorithm ND<sub>2</sub> to study is

$$375 \quad (3.23) \quad \left\{ \begin{array}{l} \left( \begin{array}{c} \dot{z}_{1,(i)}^k \\ \dot{\mu}_{1,(i)}^k \end{array} \right) + \begin{pmatrix} d_i & -\nu^{-1} \\ -1 & -d_i \end{pmatrix} \begin{pmatrix} z_{1,(i)}^k \\ \mu_{1,(i)}^k \end{pmatrix} = \begin{pmatrix} 0 \\ 0 \end{pmatrix} \text{ in } \Omega_1, \\ z_{1,(i)}^k(0) = 0, \\ \dot{z}_{1,(i)}^k(\alpha) = f_{\alpha,(i)}^{k-1}, \end{array} \right. \\ \left\{ \begin{array}{l} \left( \begin{array}{c} \dot{z}_{2,(i)}^k \\ \dot{\mu}_{2,(i)}^k \end{array} \right) + \begin{pmatrix} d_i & -\nu^{-1} \\ -1 & -d_i \end{pmatrix} \begin{pmatrix} z_{2,(i)}^k \\ \mu_{2,(i)}^k \end{pmatrix} = \begin{pmatrix} 0 \\ 0 \end{pmatrix} \text{ in } \Omega_2, \\ z_{2,(i)}^k(\alpha) = z_{1,(i)}^k(\alpha), \\ \mu_{2,(i)}^k(T) + \gamma z_{2,(i)}^k(T) = 0, \end{array} \right.$$

376 and then we update the transmission condition by

$$377 \quad (3.24) \quad f_{\alpha,(i)}^k := (1 - \theta)f_{\alpha,(i)}^{k-1} + \theta \dot{z}_{2,(i)}^k(\alpha), \quad \theta \in (0, 1).$$

378 Similar to the algorithm DN<sub>2</sub> (3.16)-(3.17), we cannot see the forward-backward struc-  
 379 ture in  $\Omega_1$  for the algorithm ND<sub>2</sub> (3.23)-(3.24). But by interpreting the Neumann con-  
 380 dition on  $z_{1,(i)}$  in terms of  $\mu_{1,(i)}$  as explained in Remark 3.1, the forward-backward  
 381 structure is again revealed through a RD type algorithm.

382 We proceed for the convergence analysis using the formulation (2.6): for  $i =$   
 383  $1, \dots, n$  and iteration index  $k = 1, 2, \dots$ , we solve

$$384 \quad (3.25) \quad \left\{ \begin{array}{l} \dot{z}_{1,(i)}^k - (d_i^2 + \nu^{-1})z_{1,(i)}^k = 0 \text{ in } \Omega_1, \\ z_{1,(i)}^k(0) = 0, \\ \dot{z}_{1,(i)}^k(\alpha) = f_{\alpha,(i)}^{k-1}, \end{array} \right. \quad \left\{ \begin{array}{l} \dot{z}_{2,(i)}^k - (d_i^2 + \nu^{-1})z_{2,(i)}^k = 0 \text{ in } \Omega_2, \\ z_{2,(i)}^k(\alpha) = z_{1,(i)}^k(\alpha), \\ \dot{z}_{2,(i)}^k(T) + d_i z_{2,(i)}^k(T) = -\gamma\nu^{-1}z_{2,(i)}^k(T), \end{array} \right.$$

385 where we still update the transmission condition by (3.24). Note that both algo-  
386 rithms (3.23) and (3.25) are of ND type.

387 Using the solutions (3.5) and the transmission condition in (3.24), we obtain

388  $A_i^k = \frac{f_{\alpha,(i)}^{k-1}}{\sigma_i \cosh(a_i)}, B_i^k = \frac{f_{\alpha,(i)}^{k-1} \tanh(a_i)/\sigma_i}{\sigma_i \cosh(b_i) + \omega_i \sinh(b_i)}$ , and we therefore get for the update con-  
389 dition (3.24)  $f_{\alpha,(i)}^k = (1 - \theta) f_{\alpha,(i)}^{k-1} - \theta f_{\alpha,(i)}^{k-1} \tanh(a_i) \frac{\sigma_i \sinh(b_i) + \omega_i \cosh(b_i)}{\sigma_i \cosh(b_i) + \omega_i \sinh(b_i)}$ .

390 **THEOREM 3.18.** *The algorithm ND<sub>2</sub> (3.23)-(3.24) converges if and only if*

391 (3.26) 
$$\rho_{ND_2} := \max_{d_i \in \lambda(A)} \left| 1 - \theta \left( 1 + \tanh(a_i) \frac{\sigma_i \tanh(b_i) + \omega_i}{\sigma_i + \omega_i \tanh(b_i)} \right) \right| < 1.$$

392 **COROLLARY 3.19.** *The algorithm ND<sub>2</sub> for  $\theta = 1$  converges if  $\alpha \leq \frac{T}{2}$ .*

393 *Proof.* Substituting  $\theta = 1$  into (3.26), we have

394 (3.27) 
$$\rho_{ND_2}|_{\theta=1} = \max_{d_i \in \lambda(A)} \left| \tanh(a_i) \frac{\sigma_i \tanh(b_i) + \omega_i}{\sigma_i + \omega_i \tanh(b_i)} \right|.$$

395 Since  $0 < \tanh(x) < 1, \forall x > 0$ , both the numerator and the denominator in (3.27)  
396 are positive. In the case where  $a_i \leq b_i$  (i.e.,  $\alpha \leq T - \alpha$ ), we have  $\tanh(a_i) \leq \tanh(b_i)$ ,  
397 and the difference between the numerator and the denominator is  $\tanh(a_i)(\omega_i +$   
398  $\sigma_i \tanh(b_i)) - (\sigma_i + \omega_i \tanh(b_i)) = \omega_i(\tanh(a_i) - \tanh(b_i)) + \sigma_i(\tanh(b_i) \tanh(a_i) - 1) <$   
399  $0$ , meaning that  $0 < \tanh(a_i) \frac{\sigma_i \tanh(b_i) + \omega_i}{\sigma_i + \omega_i \tanh(b_i)} < 1$ . This concludes the proof.  $\square$

400 As shown in Corollary 3.15, the algorithm DN<sub>2</sub> (3.16)-(3.17) with  $\theta = 1$  does  
401 not converge for  $\alpha \leq \frac{T}{2}$ , whereas the algorithm ND<sub>2</sub> (3.23)-(3.24) converges in this  
402 case. This reveals a symmetry behavior, since the only difference between these two  
403 algorithms is that we exchange the Dirichlet and the Neumann condition in the two  
404 subdomains. This symmetry is well-known for classical DN and ND algorithms.

405 **COROLLARY 3.20.** *For  $\gamma = 0$ , the algorithm ND<sub>2</sub> for  $\theta = 1$  converges for all*  
406 *initial guesses.*

407 *Proof.* This is shown in Corollary 3.19 for  $\alpha \leq \frac{T}{2}$ . If  $\alpha > \frac{T}{2}$ , i.e.  $a_i > b_i$ , then  
408  $\tanh(a_i) > \tanh(b_i)$ , and the difference between the numerator and the denominator is  
409  $\tanh(a_i)(d_i + \sigma_i \tanh(b_i)) - (\sigma_i + d_i \tanh(b_i)) = (\tanh(b_i) \tanh(a_i) - 1)(\sigma_i - d_i \tanh(a_i -$   
410  $b_i)) < 0$ , where we use the fact that  $0 < \sigma_i - d_i < \sigma_i - d_i \tanh(a_i - b_i)$ . This shows  
411 that the algorithm ND<sub>2</sub> for  $\theta = 1$  converge for  $\alpha > \frac{T}{2}$  in the case  $\gamma = 0$ .  $\square$

412 Notice that the matrix  $A$  here can be singular, in contrast to the algorithm DN<sub>1</sub>  
413 in Corollary 3.4 where non-singularity is needed for  $A$ . As in the previous section,  
414 we can still show the convergence behavior for extreme eigenvalues. If the eigenvalue  
415  $d_i = 0$ , we find

416 (3.28) 
$$\rho_{ND_2}|_{d_i=0} = \left| 1 - \theta \left( 1 + \tanh(\sqrt{\nu^{-1}}\alpha) \frac{\tanh(\sqrt{\nu^{-1}}(T-\alpha) + \gamma\sqrt{\nu^{-1}})}{1 + \gamma\sqrt{\nu^{-1}} \tanh(\sqrt{\nu^{-1}}(T-\alpha))} \right) \right|.$$

417 The expression (3.28) is very similar to (3.21): when  $\gamma = 0$ , the convergence fac-  
418 tor (3.21) becomes  $\rho_{DN_2}|_{d_i=0, \gamma=0} = |1 - \theta(1 + \coth(\sqrt{\nu^{-1}}\alpha) \coth(\sqrt{\nu^{-1}}(T - \alpha)))|$ ,  
419 whereas (3.28) becomes  $\rho_{ND_2}|_{d_i=0, \gamma=0} = |1 - \theta(1 + \tanh(\sqrt{\nu^{-1}}\alpha) \tanh(\sqrt{\nu^{-1}}(T - \alpha)))|$ .  
420 We find again the symmetry between DN<sub>2</sub> and ND<sub>2</sub>. In the case when the eigenvalue  
421 goes to infinity, using Remark 3.6, we obtain  $\lim_{d_i \rightarrow \infty} \rho_{ND_2} = |1 - 2\theta|$ , as for DN<sub>2</sub>.  
422 By equioscillating the convergence factor again for small and large eigenvalues, we

423 obtain after some computations the relaxation parameter

$$424 \quad (3.29) \quad \theta_{\text{ND}_2}^* = \frac{2}{3 + \tanh(\sqrt{\nu^{-1}}\alpha) \frac{\tanh(\sqrt{\nu^{-1}}(T-\alpha)) + \gamma\sqrt{\nu^{-1}}}{1 + \gamma\sqrt{\nu^{-1}} \tanh(\sqrt{\nu^{-1}}(T-\alpha))}}.$$

425 We thus obtain a similar result as Theorem 3.17.

426 **THEOREM 3.21.** *If we assume that the eigenvalues of  $A$  are anywhere in the inter-*  
 427 *val  $[0, \infty)$ , then the optimal relaxation parameter  $\theta_{\text{ND}_2}^*$  for the algorithm  $\text{ND}_2$  (3.23)-*  
 428 *(3.24) with  $\gamma = 0$  is given by (3.29), and satisfies  $\frac{1}{2} < \theta_{\text{ND}_2}^* < \frac{2}{3}$ .*

429 *Proof.* As for Theorem 3.17, we take the derivative of  $\rho_{\text{ND}_2}$  with respect to  
 430  $d_i$ ,  $\frac{d\rho_{\text{ND}_2}}{dd_i} = \frac{d_i\alpha}{\sigma_i \cosh^2(a_i)} \frac{\sigma_i \tanh(b_i) + \omega_i}{\sigma_i + \omega_i \tanh(b_i)} + \frac{\nu^{-1} \tanh(a_i)}{\sigma_i} \frac{\beta_i (1 - \tanh^2(b_i)) - \frac{d_i(T-\alpha)}{\cosh^2(b_i)} (\gamma^2 \nu^{-1} + 2d_i \gamma - 1)}{(\sigma_i + \omega_i \tanh(b_i))^2}$ ,  
 431 with  $\sigma_i, \omega_i$  and  $\beta_i$  defined in (2.8). For  $\gamma = 0$ , the derivative is positive and thus  $\rho_{\text{ND}_2}$   
 432 increases with  $d_i$ . Therefore  $\theta_{\text{ND}_2}^*$  is determined by equioscillation. Inserting  $\gamma = 0$   
 433 into (3.29), the denominator becomes  $3 + \tanh(\sqrt{\nu^{-1}}\alpha) \tanh(\sqrt{\nu^{-1}}(T - \alpha)) < 4$ .  $\square$

434 As for  $\text{DN}_2$  however, the monotonicity of the convergence factor  $\rho_{\text{ND}_2}$  is not guar-  
 435 anteed for  $\gamma > 0$ , and the optimal relaxation parameter  $\theta_{\text{ND}_2}^*$  may differ from (3.29).

436 **3.3. Category III.** We finally study algorithms in Category III which run only  
 437 on the state  $\mu_{(i)}$  to solve the problem (2.4), and use DN and ND techniques.

438 **3.3.1. Dirichlet-Neumann algorithm ( $\text{DN}_3$ ).** As shown in Table 1, we apply  
 439 the Dirichlet condition in  $\Omega_1$  and the Neumann condition in  $\Omega_2$ , both to the state  
 440  $\mu_{(i)}$ . For iteration index  $k = 1, 2, \dots$ , the algorithm  $\text{DN}_3$  solves

$$441 \quad (3.30) \quad \left\{ \begin{array}{l} \left( \begin{array}{c} \dot{z}_{1,(i)}^k \\ \dot{\mu}_{1,(i)}^k \end{array} \right) + \begin{pmatrix} d_i & -\nu^{-1} \\ -1 & -d_i \end{pmatrix} \left( \begin{array}{c} z_{1,(i)}^k \\ \mu_{1,(i)}^k \end{array} \right) = \begin{pmatrix} 0 \\ 0 \end{pmatrix} \text{ in } \Omega_1, \\ z_{1,(i)}^k(0) = 0, \\ \mu_{1,(i)}^k(\alpha) = f_{\alpha,(i)}^{k-1}, \\ \left( \begin{array}{c} \dot{z}_{2,(i)}^k \\ \dot{\mu}_{2,(i)}^k \end{array} \right) + \begin{pmatrix} d_i & -\nu^{-1} \\ -1 & -d_i \end{pmatrix} \left( \begin{array}{c} z_{2,(i)}^k \\ \mu_{2,(i)}^k \end{array} \right) = \begin{pmatrix} 0 \\ 0 \end{pmatrix} \text{ in } \Omega_2, \\ \dot{\mu}_{2,(i)}^k(\alpha) = \dot{\mu}_{1,(i)}^k(\alpha), \\ \mu_{2,(i)}^k(T) + \gamma z_{2,(i)}^k(T) = 0, \end{array} \right.$$

442 and we update the transmission condition by

$$443 \quad (3.31) \quad f_{\alpha,(i)}^k := (1 - \theta) f_{\alpha,(i)}^{k-1} + \theta \mu_{2,(i)}^k(\alpha), \theta \in (0, 1).$$

444 The forward-backward structure is now less present in  $\Omega_2$ , where we would expect  
 445 to have an initial condition for  $z_{2,(i)}$  instead of  $\mu_{2,(i)}$ . By using the identity of  $\mu_{(i)}$   
 446 in (2.5), we can interpret the Neumann condition  $\dot{\mu}_{2,(i)}^k(\alpha) = \dot{\mu}_{1,(i)}^k(\alpha)$  as  $d_i \dot{z}_{2,(i)}^k(\alpha) +$   
 447  $\sigma_i^2 z_{2,(i)}^k(\alpha) = d_i \dot{z}_{1,(i)}^k(\alpha) + \sigma_i^2 z_{1,(i)}^k(\alpha)$ , a Robin type condition on  $z_{2,(i)}$ . Therefore, the  
 448 algorithm  $\text{DN}_3$  can also be interpreted as a DR algorithm.

449 For the convergence analysis, it is natural to choose the interpretation in  $\mu_{(i)}$ , i.e.,  
 450 using (2.7), which gives

$$451 \quad (3.32) \quad \left\{ \begin{array}{l} \ddot{\mu}_{1,(i)}^k - \sigma_i^2 \mu_{1,(i)}^k = 0 \text{ in } \Omega_1, \\ \dot{\mu}_{(i)}^k(0) - d_i \mu_{(i)}^k(0) = 0, \\ \mu_{1,(i)}^k(\alpha) = f_{\alpha,(i)}^{k-1}, \end{array} \right. \left\{ \begin{array}{l} \ddot{\mu}_{2,(i)}^k - \sigma_i^2 \mu_{2,(i)}^k = 0 \text{ in } \Omega_2, \\ \dot{\mu}_{2,(i)}^k(\alpha) = \dot{\mu}_{1,(i)}^k(\alpha), \\ \gamma \dot{\mu}_{(i)}^k(T) + \beta_i \mu_{(i)}^k(T) = 0, \end{array} \right.$$

452 where we still update the transmission condition through (3.31). We observe that  
 453 both (3.30) and (3.32) are DN type algorithms. Proceeding as before, we obtain:

454 **THEOREM 3.22.** *The algorithm  $DN_3$  (3.30)-(3.31) converges if and only if*

$$455 \quad (3.33) \quad \rho_{DN_3} := \max_{d_i \in \lambda(A)} \left| 1 - \theta \left( 1 + \frac{\sigma_i + d_i \coth(a_i) \gamma \sigma_i \coth(b_i) + \beta_i}{\sigma_i \coth(a_i) + d_i \gamma \sigma_i + \beta_i \coth(b_i)} \right) \right| < 1.$$

456 To get more insight, we choose  $\theta = 1$  in (3.33), and find

$$457 \quad (3.34) \quad \rho_{DN_3}|_{\theta=1} = \max_{d_i \in \lambda(A)} \left| \frac{\sigma_i + d_i \coth(a_i) \gamma \sigma_i \coth(b_i) + \beta_i}{\sigma_i \coth(a_i) + d_i \gamma \sigma_i + \beta_i \coth(b_i)} \right|.$$

458 It is less clear whether  $\gamma \sigma_i + \beta_i \coth(b_i)$  is positive, since, using the definition of  $\beta_i$   
 459 and  $\sigma_i$  from (2.8), we have  $\gamma \sigma_i + \beta_i \coth(b_i) = \gamma(\sqrt{d_i^2 + \nu^{-1}} - d_i \coth(\sqrt{d_i^2 + \nu^{-1}}(T -$   
 460  $\alpha))) + \coth(\sqrt{d_i^2 + \nu^{-1}}(T - \alpha))$ , and depending on the values of  $\nu, \gamma$  and  $\alpha$ , this could  
 461 be negative. However, we can simplify (3.34) by setting  $\gamma = 0$ , and obtain:

462 **COROLLARY 3.23.** *If  $\gamma = 0$ , then the algorithm  $DN_3$  with  $\theta = 1$  converges for all*  
 463 *initial guesses.*

464 *Proof.* Substituting  $\theta = 1$  into (3.34), we have

$$465 \quad (3.35) \quad \rho_{DN_3}|_{\theta=1} = \max_{d_i \in \lambda(A)} \left| \frac{\sigma_i \tanh(a_i) + d_i}{\sigma_i + d_i \tanh(a_i)} \tanh(b_i) \right|.$$

466 Both the numerator and the denominator are positive. Using  $0 < \tanh(x) < 1$ ,  
 467  $\forall x > 0$ , we get  $(d_i + \sigma_i \tanh(a_i)) - (\sigma_i + d_i \tanh(a_i)) = (d_i - \sigma_i)(1 - \tanh(a_i)) < 0$ ,  
 468 meaning that  $0 < \tanh(b_i) \frac{\sigma_i \tanh(a_i) + d_i}{\sigma_i + d_i \tanh(a_i)} < 1$ , which concludes the proof.  $\square$

469 For  $\gamma = 0$ , the algorithm  $DN_3$  (3.30)-(3.31) converges for  $\theta = 1$  as well as the  
 470 algorithm  $ND_2$  (3.23)-(3.24), since their convergence factors are very similar. For ex-  
 471 treme eigenvalues, inserting  $d_i = 0$  into (3.33), we find the identical formula as (3.28),  
 472 and when the eigenvalue goes to infinity, we also obtain  $\lim_{d_i \rightarrow \infty} \rho_{DN_3} = |1 - 2\theta|$ . By  
 473 equioscillating the convergence factor between small and large eigenvalues, we obtain  
 474 thus the same relaxation parameter as (3.29), which leads to:

475 **THEOREM 3.24.** *If we assume the eigenvalues of  $A$  can be anywhere in the interval*  
 476  $[0, \infty)$ , *then the optimal relaxation parameter  $\theta_{DN_3}^*$  for the algorithm  $DN_3$  (3.30)-(3.31)*  
 477 *with  $\gamma = 0$  is identical to  $\theta_{ND_2}^*$ .*

478 *Proof.* For  $\gamma = 0$ , the convergence factors (3.27) and (3.35) become the same  
 479 when exchanging  $a_i$  and  $b_i$ , and the result thus follows as for Theorem 3.21.  $\square$

480 **3.3.2. Neumann-Dirichlet algorithm (ND<sub>3</sub>).** We now exchange the Dirich-  
 481 let and Neumann conditions on the two subdomains, and obtain

$$482 \quad (3.36) \quad \left\{ \begin{array}{l} \left( \begin{array}{l} \dot{z}_{1,(i)}^k \\ \dot{\mu}_{1,(i)}^k \end{array} \right) + \begin{pmatrix} d_i & -\nu^{-1} \\ -1 & -d_i \end{pmatrix} \left( \begin{array}{l} z_{1,(i)}^k \\ \mu_{1,(i)}^k \end{array} \right) = \begin{pmatrix} 0 \\ 0 \end{pmatrix} \text{ in } \Omega_1, \\ z_{1,(i)}^k(0) = 0, \\ \dot{\mu}_{1,(i)}^k(\alpha) = f_{\alpha,(i)}^{k-1}, \\ \left( \begin{array}{l} \dot{z}_{2,(i)}^k \\ \dot{\mu}_{2,(i)}^k \end{array} \right) + \begin{pmatrix} d_i & -\nu^{-1} \\ -1 & -d_i \end{pmatrix} \left( \begin{array}{l} z_{2,(i)}^k \\ \mu_{2,(i)}^k \end{array} \right) = \begin{pmatrix} 0 \\ 0 \end{pmatrix} \text{ in } \Omega_2, \\ \mu_{2,(i)}^k(\alpha) = \mu_{1,(i)}^k(\alpha), \\ \mu_{2,(i)}^k(T) + \gamma z_{2,(i)}^k(T) = 0, \end{array} \right.$$

483 where the transmission condition is updated by

$$484 \quad (3.37) \quad f_{\alpha,(i)}^k := (1 - \theta)f_{\alpha,(i)}^{k-1} + \theta\dot{\mu}_{2,(i)}^k(\alpha), \theta \in (0, 1).$$

485 As for  $\text{DN}_3$ , we need to use the identity (2.5) and interpret  $\mu_{2,(i)}^k(\alpha) = \mu_{1,(i)}^k(\alpha)$  as  
 486  $\dot{z}_{2,(i)}^k(\alpha) + d_i z_{2,(i)}^k(\alpha) = \dot{z}_{1,(i)}^k(\alpha) + d_i z_{1,(i)}^k(\alpha)$  to reveal the forward-backward structure  
 487 with a NR type algorithm. Using formulation (2.7), we get

$$488 \quad (3.38) \quad \begin{cases} \ddot{\mu}_{1,(i)}^k - \sigma_i^2 \mu_{1,(i)}^k = 0 \text{ in } \Omega_1, \\ \dot{\mu}_{(i)}^k(0) - d_i \mu_{(i)}^k(0) = 0, \\ \mu_{1,(i)}^k(\alpha) = f_{\alpha,(i)}^{k-1}, \end{cases} \quad \begin{cases} \ddot{\mu}_{2,(i)}^k - \sigma_i^2 \mu_{2,(i)}^k = 0 \text{ in } \Omega_2, \\ \mu_{2,(i)}^k(\alpha) = \mu_{1,(i)}^k(\alpha), \\ \gamma \dot{\mu}_{(i)}^k(T) + \beta_i \mu_{(i)}^k(T) = 0. \end{cases}$$

489 **THEOREM 3.25.** *The algorithm  $\text{ND}_3$  (3.36)-(3.37) converges if and only if*

$$490 \quad (3.39) \quad \rho_{\text{ND}_3} := \max_{d_i \in \lambda(A)} \left| 1 - \theta \left( 1 + \frac{\sigma_i + d_i \tanh(a_i)}{\sigma_i \tanh(a_i) + d_i} \frac{\gamma \sigma_i \tanh(b_i) + \beta_i}{\gamma \sigma_i + \beta_i \tanh(b_i)} \right) \right| < 1.$$

491 As in the previous section, we choose  $\theta = 1$  in (3.39), and find

$$492 \quad (3.40) \quad \rho_{\text{ND}_3}|_{\theta=1} = \max_{d_i \in \lambda(A)} \left| \frac{\sigma_i + d_i \tanh(a_i)}{\sigma_i \tanh(a_i) + d_i} \frac{\gamma \sigma_i \tanh(b_i) + \beta_i}{\gamma \sigma_i + \beta_i \tanh(b_i)} \right|.$$

493 Again, using the definition of  $\beta_i$  and  $\sigma_i$  from (2.8), we have  $\gamma \sigma_i \tanh(b_i) + \beta_i =$   
 494  $\gamma(\sqrt{d_i^2 + \nu^{-1}} \tanh(\sqrt{d_i^2 + \nu^{-1}}(T - \alpha)) - d_i) + 1$ , and depending on the values of  $\nu, \gamma$   
 495 and  $\alpha$ , this could be negative. However, we can simplify (3.40) by taking  $\gamma = 0$ , and  
 496 then obtain the following result.

497 **COROLLARY 3.26.** *If  $\gamma = 0$ , then the algorithm  $\text{ND}_3$  with  $\theta = 1$  does not converge.*

498 *Proof.* Inserting  $\gamma = 0$  into (3.40), we get

$$499 \quad (3.41) \quad \rho_{\text{DN}_3}|_{\theta=1} = \max_{d_i \in \lambda(A)} \left| \frac{\sigma_i \coth(a_i) + d_i}{\sigma_i + d_i \coth(a_i)} \coth(b_i) \right|.$$

500 Both the numerator and the denominator are positive. Using  $\coth(x) \geq 1, \forall x > 0$ ,  
 501 we find  $(d_i + \sigma_i \coth(a_i)) - (\sigma_i + d_i \coth(a_i)) = (\sigma_i - d_i)(\coth(a_i) - 1) > 0$ , implying  
 502 that  $\frac{\sigma_i \coth(a_i) + d_i}{\sigma_i + d_i \coth(a_i)} \coth(b_i) > 1$ , which concludes the proof.  $\square$

503 Comparing Corollaries 3.23 and 3.26, we find again a symmetry if  $\gamma = 0$ , as for  
 504 Corollaries 3.15 and 3.19, and with  $\theta = 1$ ,  $\text{ND}_3$  diverges like  $\text{DN}_2$  when  $\gamma = 0$ . In fact,  
 505 in this case, the convergence factor of  $\text{ND}_3$  (3.41) is very similar to the convergence  
 506 factor of  $\text{DN}_2$  (3.20). Due to this divergence, we cannot provide a general estimate  
 507 of the convergence factor. We can however still study the convergence behavior for  
 508 extreme eigenvalues. Inserting  $d_i = 0$  into (3.39), we find also (3.21), and thus for  
 509 small eigenvalues  $\text{ND}_3$  behaves like  $\text{DN}_2$ , like we observed for  $\text{ND}_2$  and  $\text{DN}_3$  earlier.  
 510 When the eigenvalue goes to infinity, we also obtain  $\lim_{d_i \rightarrow \infty} \rho_{\text{ND}_3} = |1 - 2\theta|$ . Hence all  
 511 the four algorithms  $\text{DN}_2, \text{ND}_2, \text{DN}_3$  and  $\text{ND}_3$  have the same limit for large eigenvalues.  
 512 By equioscillation, we then obtain the same relaxation parameter as (3.22). This leads  
 513 to a similar result as Theorem 3.17.

514 **THEOREM 3.27.** *If we assume that the eigenvalues of  $A$  are anywhere in the inter-*  
 515 *val  $[0, \infty)$ , then the optimal relaxation parameter  $\theta_{\text{ND}_3}^*$  for the algorithm  $\text{ND}_3$  (3.36)-*  
 516 *(3.37) with  $\gamma = 0$  is identical to  $\theta_{\text{DN}_2}^*$ .*

517 *Proof.* In the case  $\gamma = 0$ , the convergence factors (3.20) and (3.41) are the same  
 518 when exchanging  $a_i$  and  $b_i$ , and thus the proof follows as for Theorem 3.17.  $\square$



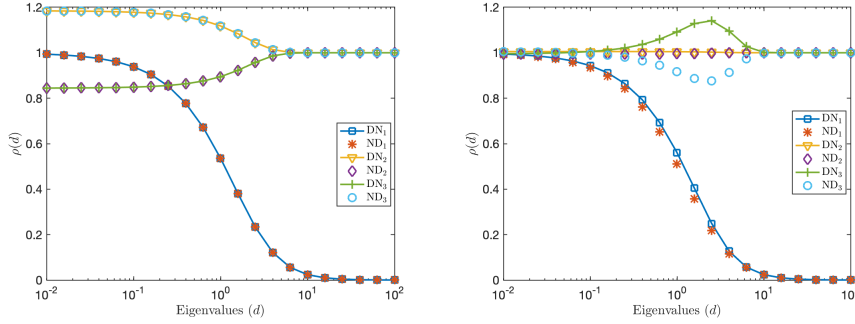


FIG. 2. Convergence factor with  $\theta = 1$  for a symmetric decomposition of the six new algorithms as function of the eigenvalues  $d \in [10^{-2}, 10^2]$ . Left:  $\gamma = 0$ . Right:  $\gamma = 10$ .

519 **4. Numerical experiments.** We illustrate now our six new time domain de-  
 520 composition algorithms with numerical experiments. We divide the time domain  
 521  $\Omega = (0, 1)$  into two non-overlapping subdomains with interface  $\alpha$ , and fix the regu-  
 522 larization parameter  $\nu = 0.1$ . We will investigate the performance by plotting the  
 523 convergence factor as function of the eigenvalues  $d \in [10^{-2}, 10^2]$ .

524 **4.1. Convergence factor with  $\theta = 1$  for a symmetric decomposition.**

525 We show in Figure 2 the convergence factors for all six algorithms for a symmetric  
 526 decomposition,  $\alpha = \frac{1}{2}$ , with  $\theta = 1$ , on the left without final target state (i.e.,  $\gamma = 0$ ),  
 527 and on the right with a final target state for  $\gamma = 10$ . Without final target state,  
 528 the convergence factor of  $DN_1$  and  $ND_1$  coincide, as one can see also by substituting  
 529  $\gamma = 0$  and  $a_i = b_i$  into (3.7) and (3.14). The same also holds for the pairs  $DN_2$  and  
 530  $ND_3$ , and  $DN_3$  and  $ND_2$ . We also see the symmetry between  $DN_2$  and  $ND_2$ , as well  
 531 as  $DN_3$  and  $ND_3$ . This changes when a final target state with  $\gamma = 10$  is present:  
 532 while the convergence behavior remains similar for  $DN_1$  and  $ND_1$ , the symmetry  
 533 between  $DN_2$  and  $ND_2$ <sup>1</sup> and  $DN_3$  and  $ND_3$  remains. Furthermore,  $DN_3$  converges  
 534 with no final target but diverges with  $\gamma = 10$ , and vice versa for  $ND_3$ . In terms of  
 535 the convergence speed,  $DN_1$  and  $ND_1$  are much better than the other four algorithms  
 536 for high frequencies in both cases, and  $ND_1$  is slightly better overall than  $DN_1$  when  
 537  $\gamma = 10$ . The good high frequency behavior follows from our analysis: it depends for  
 538 all 6 algorithms only on  $\theta$ . In the case  $\theta = 1$  here, the limit is  $|1 - \theta| = 0$  for  $DN_1$   
 539 and  $ND_1$ , and  $|1 - 2\theta| = 1$  for  $DN_2$ ,  $DN_3$ ,  $ND_2$  and  $ND_3$ . For the zero frequency,  
 540  $d = 0$ , the convergence factor for  $DN_1$  and  $ND_1$  equals 1 for all  $\gamma$ , but for  $DN_2$ ,  $DN_3$ ,  
 541  $ND_2$  and  $ND_3$  this depends on  $\gamma$ . Inserting  $\theta = 1$  into (3.21) and (3.28), we obtain  
 542 for  $DN_2$  and  $ND_3$  the convergence factor  $\frac{\coth(\sqrt{\nu^{-1}}\alpha)}{\sqrt{\nu^{-1} + \nu^{-1}\gamma \coth(\sqrt{\nu^{-1}}\alpha)}}$ , and for  
 543  $ND_2$  and  $DN_3$   $\frac{\tanh(\sqrt{\nu^{-1}}\alpha)}{\sqrt{\nu^{-1} + \nu^{-1}\gamma \tanh(\sqrt{\nu^{-1}}\alpha)}}$ . For  $\gamma = 0$ , the two convergence  
 544 factors are approximately 1.185 for  $DN_2$  and  $ND_3$ , 0.844 for  $ND_2$  and  $DN_3$ , and for  
 545  $\gamma = 10$ , we get 1.005 for  $DN_2$  and  $ND_3$ , and 0.995  $ND_2$  and  $DN_3$ .

546 **4.2. Convergence factor with  $\theta = 1$  for an asymmetric decomposition.**

547 For  $\theta = 1$ , we show on the left in Figure 3 the convergence factors with interface at  
 548  $\alpha = 0.3$  and no final target state (i.e.,  $\gamma = 0$ ), and on the right  $\alpha = 0.7$  with a final

<sup>1</sup>This is a bit hard to see on the right in Figure 2, but zooming in confirms that the convergence factor of  $DN_2$  is above 1, and below 1 for  $ND_2$ .

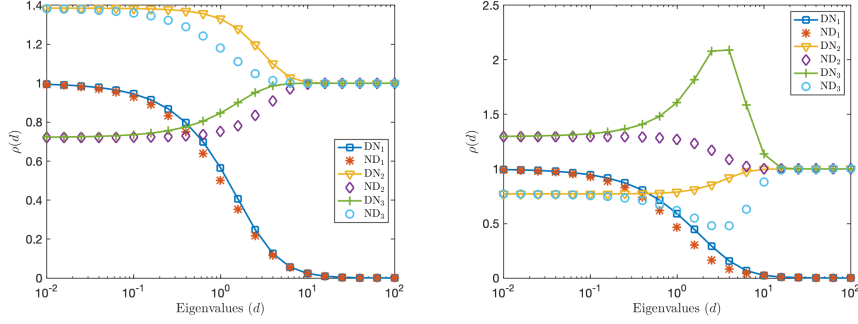


FIG. 3. Convergence factor with  $\theta = 1$  for an asymmetric decomposition of all six new algorithms as function of the eigenvalues  $d \in [10^{-2}, 10^2]$ . Left:  $\gamma = 0$  and  $\alpha = 0.3$ . Right:  $\gamma = 10$  and  $\alpha = 0.7$ .

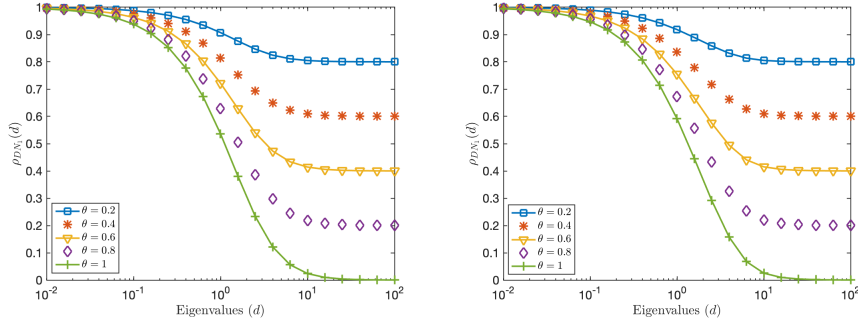


FIG. 4. Convergence factor with different relaxation parameters of  $DN_1$  as function of the eigenvalues  $d \in [10^{-2}, 10^2]$ . Left:  $\gamma = 0$  and  $\alpha = 0.5$ . Right:  $\gamma = 10$  and  $\alpha = 0.7$ .

549 target state  $\gamma = 10$ . For  $DN_1$  and  $ND_1$ , the convergence factor is similar in both  
 550 cases,  $ND_1$  being slightly better, and convergence is also similar to the symmetric  
 551 case. This is because the convergence factor of the two algorithms for small and  
 552 large eigenvalues is independent of the values of  $\alpha, \nu$  and  $\gamma$ . Their high frequency  
 553 behavior is also much better compared to the other four algorithms in the two cases.  
 554 For the other four algorithms, we see again the symmetry between  $DN_2$  and  $ND_2$ ,  
 555 and  $DN_3$  and  $ND_3$ . In general,  $DN_2$  and  $ND_3$  behave similarly, and also  $ND_2$  and  
 556  $DN_3$ , but the influence of  $\gamma$  is more significant for  $DN_3$  and  $ND_3$  than  $DN_2$  and  
 557  $ND_2$ . However their convergence factors all go to 1 for large eigenvalues, as for the symmetric  
 558 decomposition. For the zero frequency, using the expressions (3.21) and (3.28) with  
 559  $\theta = 1$ , we obtain approximately 1.386 for  $DN_2$  and  $ND_3$ , and 0.722 for  $ND_2$  and  $DN_3$   
 560 in the case  $\gamma = 0$ ,  $\alpha = 0.3$ . For  $\gamma = 10$ ,  $\alpha = 0.7$ , we get 0.771 for  $DN_2$  and  $ND_3$ , and  
 561 1.296 for  $ND_2$  and  $DN_3$ .

562 **4.3. Convergence factor for Category I with different  $\theta$ .** Since  $DN_1$  and  
 563  $ND_1$  performed quite similarly, and much better than the others, we now investigate  
 564 the dependence of  $DN_1$  on  $\theta$  in more detail. On the left in Figure 4 we show the  
 565 convergence factor of  $DN_1$  without final target state and a symmetric decomposition,  
 566 and on the right with a final target state  $\gamma = 10$  and an asymmetric decomposition.  
 567 The convergence is very similar for these two settings,  $DN_1$  is robust, and  $\theta = 1$  gives  
 568 the best performance.

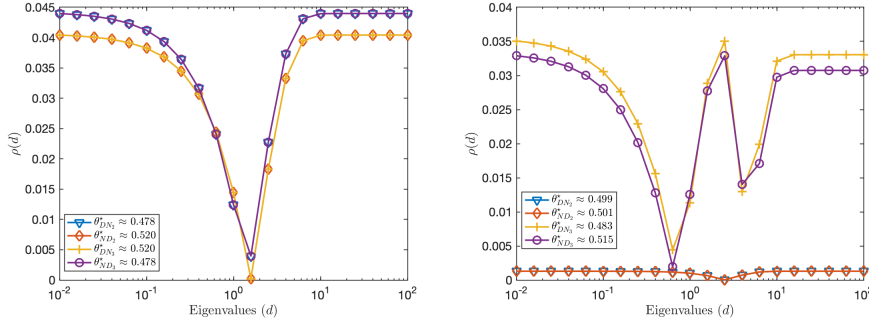


FIG. 5. Convergence factor with  $\theta^*$  for a symmetric decomposition as function of the eigenvalues  $d \in [10^{-2}, 10^2]$ . Left:  $\gamma = 0$ . Right:  $\gamma = 10$ .

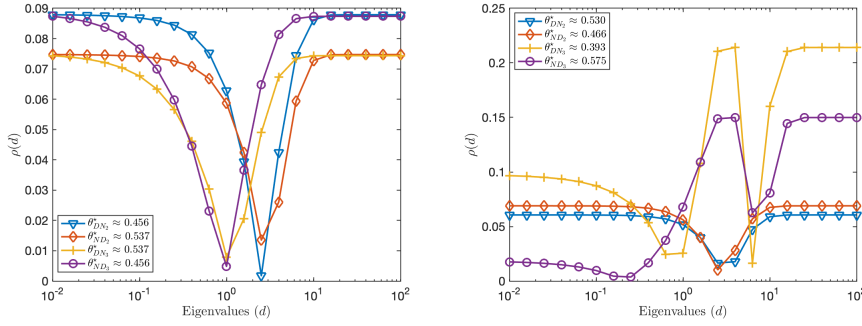


FIG. 6. Convergence factor with  $\theta^*$  for an asymmetric decomposition as function of the eigenvalues  $d \in [10^{-2}, 10^2]$ . Left:  $\gamma = 0$  and  $\alpha = 0.3$ . Right:  $\gamma = 10$  and  $\alpha = 0.7$ .

569 **4.4. Convergence factor with optimal  $\theta$  for a symmetric decomposi-**  
 570 **tion.** Since the algorithms in Categories II and III are strongly related, we compare  
 571 them now in Figure 5 for a symmetric decomposition using their optimal relaxation  
 572 parameter  $\theta^*$ , obtained numerically. On the left without final state, DN<sub>2</sub> and ND<sub>3</sub>,  
 573 and also ND<sub>2</sub> and DN<sub>3</sub>, have the same convergence factor, and the optimal relaxa-  
 574 tion parameter satisfies  $\theta_{\text{DN}_2}^* = \theta_{\text{ND}_3}^*$  and  $\theta_{\text{ND}_2}^* = \theta_{\text{DN}_3}^*$  as proved in Theorem 3.24  
 575 and Theorem 3.27. These correspond to the value found using (3.22) and (3.29). In  
 576 terms of the convergence speed, ND<sub>2</sub> and DN<sub>3</sub> are slightly better than DN<sub>2</sub> and ND<sub>3</sub>.  
 577 However, these similarities disappear when we add a final target state  $\gamma = 10$ . On  
 578 the right in Figure 5, we see that now the convergence behavior of DN<sub>2</sub> and ND<sub>2</sub>  
 579 is similar, and also DN<sub>3</sub> and ND<sub>3</sub> are rather similar, and DN<sub>2</sub> and ND<sub>2</sub> converge  
 580 much faster compared to the others. We also see equioscillation between small and  
 581 large eigenvalues. The theoretical results in (3.22) as well as in (3.29) still determine  
 582 the optimal relaxation parameter  $\theta_{\text{DN}_2}^*$  and  $\theta_{\text{ND}_2}^*$  for DN<sub>2</sub> and ND<sub>2</sub>, but not for DN<sub>3</sub>  
 583 and ND<sub>3</sub>, where we observe an equioscillation between small eigenvalues with some  
 584 eigenvalues in the interval  $[1, 10]$ . Also ND<sub>3</sub> is slightly better than DN<sub>3</sub>.

585 **4.5. Convergence factor with optimal  $\theta$  for an asymmetric decomposi-**  
 586 **tion.** We show in Figure 6 the convergence factor with the optimal relaxation param-  
 587 eter  $\theta^*$  for the four algorithms in Categories II and III for an asymmetric decomposition.  
 588 On the left with  $\alpha = 0.3$  and no target state  $\gamma = 0$  the convergence factors of the four

589 algorithms are similar. This is consistent with the monotonicity we proved without  
 590 final state. The optimal relaxation parameters satisfy  $\theta_{\text{DN}_2}^* = \theta_{\text{ND}_3}^*$  and  $\theta_{\text{ND}_2}^* = \theta_{\text{DN}_3}^*$ ,  
 591 and we can use (3.22) and (3.29) to determine their values. Similar to the symmetric  
 592 decomposition,  $\text{ND}_2$  and  $\text{DN}_3$  are slightly better than the others. However, these  
 593 properties disappear again on the right in Figure 6 when there is a final state  $\gamma = 10$ .  
 594 While  $\text{DN}_2$  and  $\text{ND}_2$  still equioscillate between the small and large eigenvalues, and  
 595 the optimal relaxation parameter can be determined using (3.22) and (3.29), for  $\text{DN}_3$   
 596 and  $\text{ND}_3$  the equioscillation is between large eigenvalues and some eigenvalues in the  
 597 interval  $[1, 10]$ . Hence, the optimal relaxation parameters for the algorithms  $\text{DN}_3$  and  
 598  $\text{ND}_3$  are different from  $\text{DN}_2$  and  $\text{ND}_2$ . Also  $\text{DN}_2$  and  $\text{ND}_2$  converge much faster than  
 599 the other two, and  $\text{DN}_2$  is slightly faster than  $\text{ND}_2$ .

600 **5. Conclusion.** We introduced and analyzed six new time domain decompo-  
 601 sition methods based on Dirichlet-Neumann and Neumann-Dirichlet techniques for  
 602 parabolic optimal control problems. Our analysis shows that while at first sight it  
 603 might be natural to preserve the forward-backward structure in the time subdomains  
 604 as well, there are better choices that lead to substantially faster algorithms. We find  
 605 that the algorithms in Categories II and III with optimized relaxation parameter are  
 606 much faster than the algorithms in Category I, and they can still be identified to be  
 607 of forward-backward structure using changes of variables. We also found many inter-  
 608 esting mathematical connections between these algorithms. Algorithms in Category  
 609 I are natural smoothers, while algorithms in Categories II and III with optimized  
 610 relaxation parameter are highly efficient solvers.

611 Our study was restricted to the two subdomain case, but the algorithms can all  
 612 naturally be written for many subdomains, and then one can also run them in parallel.  
 613 They can also be used for more general parabolic constraints than the heat equation.  
 614 Extensive numerical results will appear elsewhere.

615

## REFERENCES

- 616 [1] R. A. BARTLETT, M. HEINKENSCHLOSS, D. RIDZAL, AND B. G. VAN BLOEMEN WAANDERS,  
 617 *Domain decomposition methods for advection dominated linear-quadratic elliptic optimal*  
 618 *control problems*, Computer Methods in Applied Mechanics and Engineering, 195 (2006),  
 619 pp. 6428–6447, <https://doi.org/10.1016/j.cma.2006.01.009>.  
 620 [2] J.-D. BENAMOU, *A domain decomposition method with coupled transmission conditions for*  
 621 *the optimal control of systems governed by elliptic partial differential equations*, SIAM  
 622 *Journal on Numerical Analysis*, 33 (1996), pp. 2401–2416, [https://doi.org/10.1137/](https://doi.org/10.1137/S0036142994267102)  
 623 [S0036142994267102](https://doi.org/10.1137/S0036142994267102).  
 624 [3] P. E. BJØRSTAD AND O. B. WIDLUND, *Iterative methods for the solution of elliptic problems*  
 625 *on regions partitioned into substructures*, SIAM Journal on Numerical Analysis, 23 (1986),  
 626 pp. 1097–1120, <https://doi.org/10.1137/0723075>.  
 627 [4] A. BORZI AND V. SCHULZ, *Computational Optimization of Systems Governed by Partial*  
 628 *Differential Equations*, Society for Industrial and Applied Mathematics, 2011, <https://doi.org/10.1137/1.9781611972054>.  
 629 [5] H. CHANG AND D. YANG, *A Schwarz domain decomposition method with gradient projection for*  
 630 *optimal control governed by elliptic partial differential equations*, Journal of Computational  
 631 and Applied Mathematics, 235 (2011), pp. 5078–5094, [https://doi.org/10.1016/j.cam.2011.](https://doi.org/10.1016/j.cam.2011.04.037)  
 632 [04.037](https://doi.org/10.1016/j.cam.2011.04.037).  
 633 [6] G. CIARAMELLA, L. HALPERN, AND L. MECHELLI, *Convergence analysis and optimization of*  
 634 *a robin schwarz waveform relaxation method for time-periodic parabolic optimal control*  
 635 *problems*, Journal of Computational Physics, 496 (2024), p. 112572, [https://doi.org/10.](https://doi.org/10.1016/j.jcp.2023.112572)  
 636 [1016/j.jcp.2023.112572](https://doi.org/10.1016/j.jcp.2023.112572).  
 637 [7] V. DOLEAN, P. JOLIVET, AND F. NATAF, *An Introduction to Domain Decomposition Meth-*  
 638 *ods: Algorithms, Theory, and Parallel Implementation*, Society for Industrial and Applied  
 639 Mathematics, Philadelphia, PA, 2015, <https://doi.org/10.1137/1.9781611974065>.  
 640

- 641 [8] M. J. GANDER AND F. KWOK, *Schwarz methods for the time-parallel solution of para-*  
 642 *abolic control problems*, in Domain Decomposition Methods in Science and Engineering  
 643 XXII, T. Dickopf, M. J. Gander, L. Halpern, R. Krause, and L. F. Pavarino, eds.,  
 644 Cham, 2016, Springer International Publishing, pp. 207–216, [https://doi.org/10.1007/](https://doi.org/10.1007/978-3-319-18827-0_19)  
 645 [978-3-319-18827-0\\_19](https://doi.org/10.1007/978-3-319-18827-0_19).
- 646 [9] M. J. GANDER, F. KWOK, AND B. C. MANDAL, *Convergence of substructuring methods for*  
 647 *elliptic optimal control problems*, in Domain Decomposition Methods in Science and  
 648 Engineering XXIV, Cham, 2019, Springer International Publishing, pp. 291–300, [https://doi.org/10.1007/978-3-319-93873-8\\_27](https://doi.org/10.1007/978-3-319-93873-8_27).  
 649
- 650 [10] M. J. GANDER, F. KWOK, AND J. SALOMON, *Paraopt: A parareal algorithm for optimality*  
 651 *systems*, SIAM Journal on Scientific Computing, 42 (2020), pp. A2773–A2802, <https://doi.org/10.1137/19M1292291>.  
 652
- 653 [11] M. J. GANDER, F. KWOK, AND G. WANNER, *Constrained Optimization: From Lagrangian*  
 654 *Mechanics to Optimal Control and PDE Constraints*, Springer International Publishing,  
 655 Cham, 2014, pp. 151–202, [https://doi.org/10.1007/978-3-319-08025-3\\_5](https://doi.org/10.1007/978-3-319-08025-3_5).
- 656 [12] M. J. GANDER AND A. M. STUART, *Space-time continuous analysis of waveform relaxation*  
 657 *for the heat equation*, SIAM Journal on Scientific Computing, 19 (1998), pp. 2014–2031,  
 658 <https://doi.org/10.1137/S1064827596305337>.
- 659 [13] M. HEINKENSCHLOSS, *A time-domain decomposition iterative method for the solution of dis-*  
 660 *tributed linear quadratic optimal control problems*, Journal of Computational and Applied  
 661 Mathematics, 173 (2005), pp. 169–198, <https://doi.org/10.1016/j.cam.2004.03.005>.
- 662 [14] M. HINZE, R. PINNAU, M. ULBRICH, AND S. ULBRICH, *Optimization with PDE Constraints*,  
 663 Springer Dordrecht, 2009, <https://doi.org/10.1007/978-1-4020-8839-1>.
- 664 [15] F. KWOK, *On the time-domain decomposition of parabolic optimal control problems*, in Domain  
 665 Decomposition Methods in Science and Engineering XXIII, C.-O. Lee, X.-C. Cai, D. E.  
 666 Keyes, H. H. Kim, A. Klawonn, E.-J. Park, and O. B. Widlund, eds., Cham, 2017, Springer  
 667 International Publishing, pp. 55–67, [https://doi.org/10.1007/978-3-319-52389-7\\_5](https://doi.org/10.1007/978-3-319-52389-7_5).
- 668 [16] U. LANGER, O. STEINBACH, F. TRÖLTZSCH, AND H. YANG, *Space-time finite element discretiza-*  
 669 *tion of parabolic optimal control problems with energy regularization*, SIAM Journal on  
 670 Numerical Analysis, 59 (2021), pp. 675–695, <https://doi.org/10.1137/20M1332980>.
- 671 [17] E. LELARSMEE, A. RUEHLI, AND A. SANGIOVANNI-VINCENTELLI, *The waveform relaxation*  
 672 *method for time-domain analysis of large scale integrated circuits*, IEEE Transactions on  
 673 Computer-Aided Design of Integrated Circuits and Systems, 1 (1982), pp. 131–145, <https://doi.org/10.1109/TCAD.1982.1270004>.  
 674
- 675 [18] J.-L. LIONS, *Optimal Control of Systems Governed by Partial Differential Equations*, 170,  
 676 Springer-Verlag Berlin Heidelberg, 1 ed., 1971.
- 677 [19] J.-L. LIONS, Y. MADAY, AND G. TURINICI, *A parareal in time procedure for the control of*  
 678 *partial differential equations*, Comptes Rendus Mathématique, 335 (2002), pp. 387–392,  
 679 [https://doi.org/10.1016/S1631-073X\(02\)02467-6](https://doi.org/10.1016/S1631-073X(02)02467-6).
- 680 [20] C. LUBICH AND A. OSTERMANN, *Multi-grid dynamic iteration for parabolic equations*, BIT  
 681 Numerical Mathematics, 27 (1987), pp. 216–234, <https://doi.org/10.1007/BF01934186>.
- 682 [21] B. C. MANDAL, *Substructuring waveform relaxation methods for parabolic optimal control*  
 683 *problems*, in Soft Computing for Problem Solving, J. C. Bansal, K. N. Das, A. Na-  
 684 gar, K. Deep, and A. K. Ojha, eds., Singapore, 2019, Springer Singapore, pp. 485–494,  
 685 [https://doi.org/10.1007/978-981-13-1595-4\\_39](https://doi.org/10.1007/978-981-13-1595-4_39).
- 686 [22] W. L. MIRANKER AND W. LINIGER, *Parallel methods for the numerical integration of ordinary*  
 687 *differential equations*, Mathematics of Computation, 21 (1967), pp. 303–320, <https://doi.org/10.2307/2003233>.  
 688
- 689 [23] M. NEUMÜLLER AND O. STEINBACH, *Regularization error estimates for distributed control prob-*  
 690 *lems in energy spaces*, Mathematical Methods in the Applied Sciences, 44 (2021), pp. 4176–  
 691 4191, <https://doi.org/10.1002/mma.7021>.
- 692 [24] J. NIEVERGELT, *Parallel methods for integrating ordinary differential equations*, Commun.  
 693 ACM, 7 (1964), p. 731–733, <https://doi.org/10.1145/355588.365137>.
- 694 [25] A. TOSELLI AND O. B. WIDLUND, *Domain Decomposition Methods - Algorithms and Theory*,  
 695 Springer Berlin, Heidelberg, 1 ed., 2005, <https://doi.org/10.1007/b137868>.
- 696 [26] F. TRÖLTZSCH, *Optimal Control of Partial Differential Equations: Theory, Methods and Ap-*  
 697 *plications*, vol. 112, Graduate Studies in Mathematics, 2010, [https://doi.org/10.1090/gsm/](https://doi.org/10.1090/gsm/112)  
 698 [112](https://doi.org/10.1090/gsm/112).
- 699 [27] S. VANDEWALLE AND E. VELDE, *Space-time concurrent multigrid waveform relaxation*, Annals  
 700 of Numerical Mathematics, 1-4 (1994), pp. 347–363, [https://doi.org/10.13140/2.1.1146.](https://doi.org/10.13140/2.1.1146.1761)  
 701 [1761](https://doi.org/10.13140/2.1.1146.1761).

## 702 Appendix A. Convergence analysis using $\mu_{(i)}$ .

703 We can also use formulation (2.7) to analyze the convergence behavior of the  
704 algorithm  $\text{DN}_1$  (3.1)-(3.2), we then need to study

(A.1)

$$705 \quad \begin{cases} \ddot{\mu}_{1,(i)}^k - \sigma_i^2 \mu_{1,(i)}^k = 0 \text{ in } \Omega_1, \\ \dot{\mu}_{(i)}^k(0) - d_i \mu_{(i)}^k(0) = 0, \\ \mu_{1,(i)}^k(\alpha) = f_{\alpha,(i)}^{k-1}, \end{cases} \quad \begin{cases} \ddot{\mu}_{2,(i)}^k - \sigma_i^2 \mu_{2,(i)}^k = 0 \text{ in } \Omega_2, \\ \ddot{\mu}_{2,(i)}^k(\alpha) - d_i \mu_{2,(i)}^k(\alpha) = \ddot{\mu}_{1,(i)}^k(\alpha) - d_i \mu_{1,(i)}^k(\alpha), \\ \gamma \dot{\mu}_{(i)}^k(T) + \beta_i \mu_{(i)}^k(T) = 0, \end{cases}$$

706 with the update of the transmission condition

707 (A.2) 
$$f_{\alpha,(i)}^k = (1 - \theta) f_{\alpha,(i)}^{k-1} + \theta \mu_{2,(i)}^k(\alpha) \quad \theta \in (0, 1).$$

708 This is a DR type algorithm applied to solve (2.7). Using (3.12), we determine the  
709 two coefficients  $A_i^k$  and  $B_i^k$  from the transmission condition from (A.1). Using then  
710 relation (A.2), we find

711 
$$f_{\alpha,(i)}^k = (1 - \theta) f_{\alpha,(i)}^{k-1} + \theta \nu^{-1} f_{\alpha,(i)}^{k-1} \frac{\gamma \sigma_i + \beta_i \tanh(b_i)}{(\sigma_i + d_i \tanh(a_i))(\omega_i + \sigma_i \tanh(b_i))},$$

712 which is exactly the same convergence factor as (3.6).

713 **Appendix B. 1D Advection-diffusion problems.** We can also consider the  
714 operator  $\partial_x - \kappa \partial_{xx}$ , and use a finite difference scheme to discretize it, for instance, an  
715 upwind discretization for the advection part  $\partial_x$  and the standard centred discretization  
716 for the diffusion part  $\partial_{xx}$ . With mesh size  $h$ , the eigenfunctions in this case are  $e^{in\pi jh}$   
717 with eigenvalues  $d_n := 2(\frac{1}{h} + \kappa \frac{2}{h^2}) \sin^2(\frac{n\pi h}{2}) + i \frac{1}{h} \sin(n\pi h)$ . As presented in Section 4,  
718 we can then check the convergence behavior of the proposed algorithms for advection-  
719 diffusion problems. As an example, we keep the same setting as for Figure 5, but  
720 now use the eigenvalues from above. We show in Figure 7 the convergence factor with  
721 respect to the eigenvalues for diffusion coefficient  $\kappa = 10^{-1}$  and  $\kappa = 10^{-2}$ . Comparing  
722 with the pure diffusion case in Figure 5, we see that adding an advection term leads  
723 to slower convergence, while the order from best to worst algorithm is maintained as  
724 for pure diffusion, both for  $\gamma = 0$  (left) and  $\gamma = 10$  (right). For  $\gamma = 10$ , the slower  
725 algorithm variants even tend to stagnate as the problem becomes advection dominant,  
726 but the fast algorithms remain fast in that case, see Figure 5 (right). We also see that  
727 the optimized relaxation parameters depend on the presence of advection.

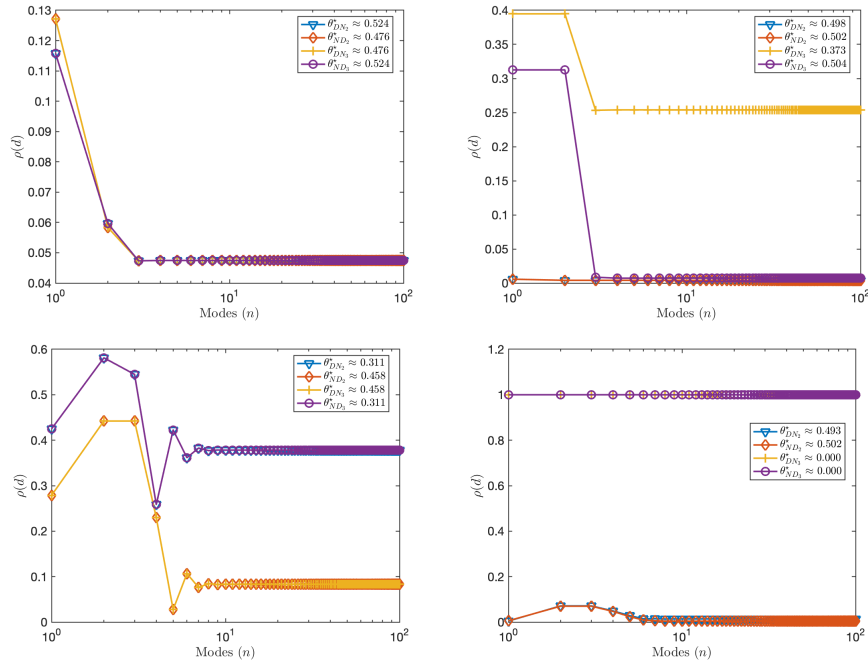


FIG. 7. Convergence factor with  $\theta^*$  for a symmetric decomposition as function of the eigenvalues  $d_n = 2(\frac{1}{h} + \kappa \frac{2}{h^2}) \sin^2(\frac{n\pi h}{2}) + i \frac{1}{h} \sin(n\pi h)$ ,  $n \in [10^0, 10^2]$ . Top:  $\kappa = 10^{-1}$ . Bottom:  $\kappa = 10^{-2}$ . Left:  $\gamma = 0$ . Right:  $\gamma = 10$ .